University of BRISTOL

‘Self assembly of Diamond Nanoparticles on Metal Electrodes’

A review of the chemical self-assembly technique and its application to diamond coated electrodes for chemical, electronic and biological applications.

Document Properties

Dissertation submitted in accordance to obtaining a BSci in Chemistry at the University of Bristol

Author – Giles Newton

Acknowledgements

My utmost gratitude must go to Dr Neil Fox, Professor Paul May, and Dr Daniela Plana for their unwavering and patient guidance through the fields of semiconducting diamond and electrochemistry. Thanks must also go to Dr David Fermin for his electrochemical inspiration and to Dr Wiphada Hongthani who led the way in revising a self-assembly technique for diamond nanoparticles on metal substrates.

Abstract

Chemical self-assembly is a 'bottom up' technique describing the spontaneous ordering of molecules onto a substrate. This technique was used to assemble semi-conducting diamond nanoparticles onto Tungsten and Tantalum substrates in order to undergo testing for thermionic emission. A branch of self-assembly, which in the authors best knowledge, has not been conducted outside this research group. Tungsten and Tantalum were chosen to take advantage of their superior thermal stability and low expansion coefficient (4.5μm m^{-1} K^{-1}).

High pressure high temperature nanodiamond, of nominal size 500nm, was used in the self-assembly process. It has previously been found difficult to assemble particles of less than 500nm on metal substrates. In this review the self-assembly technique was refined in an attempt to work with particles of less than 450nm.

Oxygenation of diamond nanoparticles is known to induce a positive electron affinity onto the diamond surface, causing downward band bending. Positive electron affinity is also important in inducing auxiliary negative electron affinity surfaces. Oxygenation of diamond nanoparticles was attempted electrochemically at high potentials on ITO electrodes. Electrochemical hydrogenation was also attempted in the hope of forming a comparison between the two diamond surfaces via SEM analysis.

Contents

1.0 Introduction....4
2.0 Self-Assembly....5
2.1 Self-Assembled Monolayers....7
3.0 Diamond Nanoparticles (DNPs)....10
3.1 Synthesis of DNPs....10
3.2 Properties of Diamond Nanoparticles....11
3.3 P-type and N-type Doping of Diamond Nanoparticles....12
3.4 Surface Termination of DNPs....13
4.0 Self-Assembled Diamond Monolayers....15
4.1 Applications of DNPs....15
4.2 Conducting DNPs and their Applications....17
4.2.1 Electronic Applications....17
4.2.2 Catalytic Applications....19
4.3 Self-Assembly of DNPs to Electrodes and Corresponding Analytical Applications....19
5.0 Thermionic Energy Conversion....21
6.0 Electrochemistry of Diamond....23
7.0 Experimental Techniques....24
7.1 Self-Assembly....24
7.2 Optical (Nomarski) Microscope Technique....24
7.3 SEM....25
7.4 Cyclic Voltammetry....25
8.0 Results and Discussions....26
8.1 Self-Assembly Analysis....26
8.2 Particle Size Definition....28
8.3 Electrochemical Oxidation of DNPs....31
9.0 Conclusions....35
10.0 Further Work....36
11.0 Appendices....37
12.0 Referencing....41

1.0 Introduction

Self-assembly is a useful technique that encompasses an extensive range of chemistry. Offering the ability to assemble nano-scale layers onto substrate surfaces. Chemical self-assembly is a very versatile technique and the source of a number of applications; the technique first demonstrated by Irving Langmuir (1932)[1] (shown in Fig.1) has developed rapidly and is now widely used. Recently the self-assembly of diamond onto substrate surfaces has emerged as a field of considerable interest. This interest has stemmed from the especially desirable characteristics of diamond, namely its chemical stability, rigidity, high thermal conductivity, low thermal expansion, and its electrical insulating properties[2 3 4].

The first documented interest in nanodiamond was in the 1960s by Russian scientists for military based research projects[5]. They focused on detonation nanodiamond residues, and it was only until the 1980s that other researchers picked up on the potential uses of nanodiamond. The interest and importance stemming from these nanodiamond residues is based on the word 'nano'. Nano as a prefix means 'a billionth of' to put that into scale a human hair is ~80,000nm in thickness[6]. In 1959 at a meeting of the American Physical Society, Richard Feynman was heard to say "There's plenty of room at the bottom"[7], encouraging widespread interest in nanotechnology. However it was Professor Norio Taguchi, in 1974[8], who coined the term nanotechnology. Nowadays nanotechnology is one of the fastest growing research curiosities and has revolutionized many fields such as electronic devices, the energy sector, manufacturing, and pharmaceuticals.

The self-assembly of diamond onto substrates has lead to a large range of applications including protein separation and purification, drug delivery, and biomarkers[9]. However the range of applications can be increased *via* surface modification; the use of doping techniques and specific surface terminations to make diamond semi-conducting can expand the uses of diamond thin films to include field effect transistors[10], nanoelectromechanical systems[11] such as chemical sensors, and quantum computing[12].

However in this review the most fascinating use of semi-conducting diamond is in thermionic energy emission, which has the potential to become a widespread phenomenon. The theory behind thermionic emission is the heat-induced flow of charge carriers across a surface. The charge carriers are subjected to an increase in thermal energy, which releases them from their binding potential. This induced flow of charge carriers, implies that these devices have the ability to convert heat energy in electrical energy, the applications of which could have a large bearing on future of efficient and renewable energy.

2.0 Self-Assembly

The self-assembly technique has been defined as the spontaneous ordering of molecules onto a surface by attractive forces or chemical bond formation[13] for example the hydrophilic head group of Sodium alkyl propoxylated sulfate (Fig.2) will be attracted to water, whereas the hydrophobic tail will repel away from the water leaving an ordered monolayer (a layer one molecule in width). Layer after layer can be deposited onto the surface leaving a series of monolayers, otherwise known as self-assembled monolayers (SAMs). Self-assembly is nowadays an extremely important practice, the ability to highly order and functionalize ultra-thin monolayers allows for a number of practical applications.

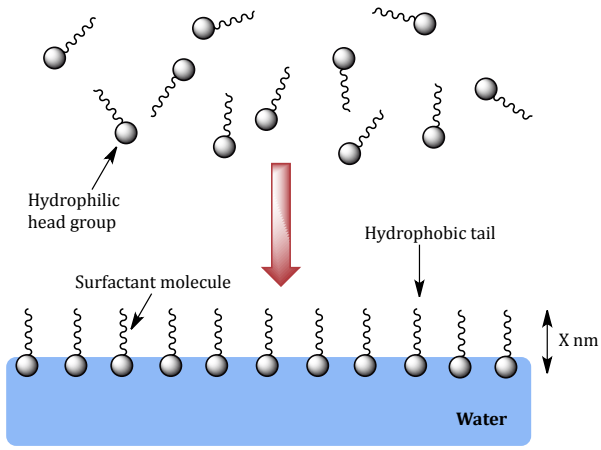

Figure 1 *shows the first stage of the Langmuir-Blodgett technique; the simple self-assembly of a surfactant monolayer: Amphiphilic molecules, such as surfactants, with hydrophilic head groups and hydrophobic tails adsorb onto a polar solvent, such as water. The ordered layer has an easily calculated thickness as the size of the surfactant particle is known. The hydrophilic head group is attracted/adsorbed onto the water surface, where as the tail repels the water strongly and forces itself away from the surface leaving the ordered film of X nm.*

One of the original examples of self-assembly is found in nature, biominerlization. Biomineralization describes how multicellular organisms create minerals and organic polymers in order to help strengthen shells and bones. Normal cellular processes form the minerals, which then replicate to give perfectly ordered structures such as bacteria, algae, and the osteoblasts of bone. In all these structures inorganic crystals are self-assembled in an ordered pattern that matches a matrix of organic macromolecules[14,15]. Biomineralization displays some highly desirable properties, such as precise structural organization, that would be of great use if synthetically available. For example silk produced by spiders displays a unique set of properties, a processable liquid crystalline phase is assembled by non-covalent aggregation of the polymer fibroin with a random coil conformation, this structure produces incredibly strong, flexible and highly compliant fibers[16].

As L. Addadi noted, it is possible to use the design principles shown in biomineralization and apply them in the fabrication of superior synthetic materials[17], experimentally mimicking

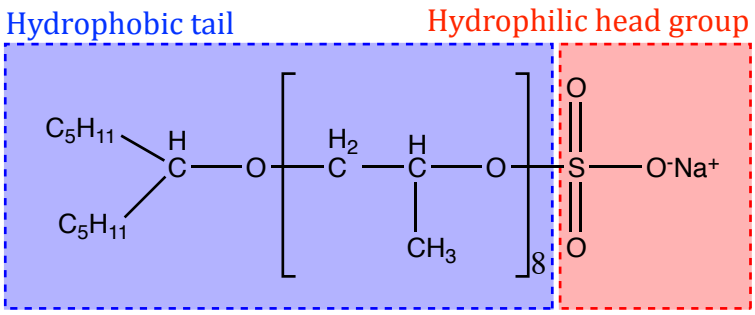

Figure 2 *– Sodium alkyl propoxylated sulfate an organic surfactant molecule. It has an easily calculated length, which is therefore equal to the width of the monolayer formed by the surfactant molecule.*

the *in situ* method of mineral formation to assemble monomolecular layers in an ordered matrix.

Irving Langmuir was one of the first people that managed to replicate nature's examples of self-assembly when he discovered the earliest form of synthesizing ultra-thin films. The well renowned self-assembly technique is now known as the Langmuir-Blodgett technique. Langmuir created the technique with the help of Katherine Blodgett; he was awarded the Nobel Prize for Chemistry in 1932[18] for his work on surface chemistry. It was previously believed that the theory behind adsorption onto a surface was that the gas or condensation was at its most dense closest to the surface and that the density of the gas decreased with distance from the surface.

Langmuir proved experimentally that molecules assembled themselves as monomolecular layers (monolayers) onto the surface and could be built outwards layer by layer. He also explained how these monomolecular layers formed ordered structures satisfying each atom's valences. The Langmuir-Blodgett technique is a way of fabricating organic molecules (or surfactants) into an extremely thin layer of uniform thickness with specific internal structure[19 20 21].

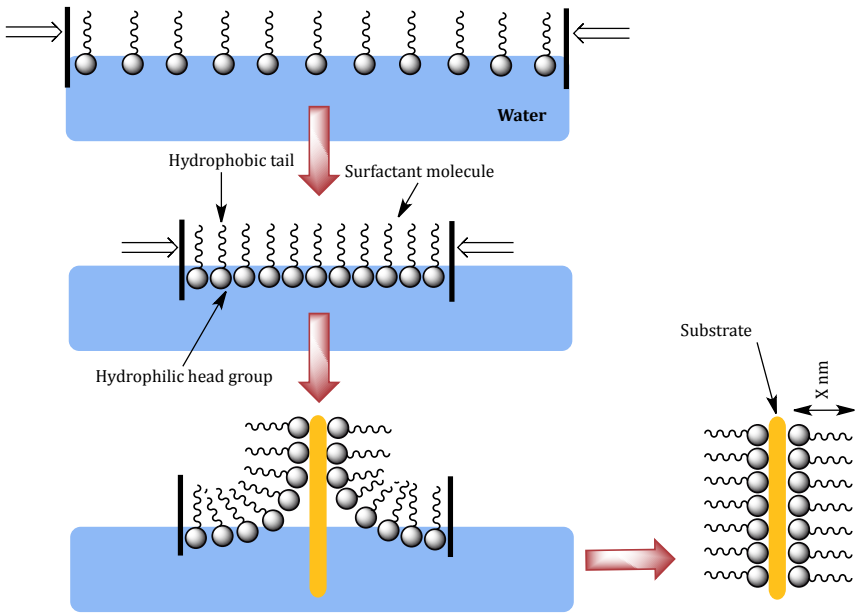

Figure 3 *displays the subsequent stages in the formation of a Langmuir-Blodgett film. Where the surfactant is deposited onto the flat substrate surface. The well-ordered monolayer is transferred from the surface of the liquid onto the surface of the substrate.*

The first step of the Langmuir-Blodgett technique is shown and described in Figure 1. Here the hydrophobic head groups of the surfactant are adsorbed onto a water surface. A strong anistropic interaction of the water molecules with the head group ensures they'll be properly bound to the surface and have no tendency to more than one layer[22]. It is important not to exceed the critical micelle concentration (CMC) where surfactant molecules will start binding together to make spherical micelles. The surfactants are spread loosely over the water surface, so the surface area has to be reduced in order for the surfactant to be more closely packed. An upward stroke from a hydrophilic substrate e.g. a flat silicon substrate, the hydrophilic

surfactant head group is adsorbs onto the surfactant, exposing the surfactant tail group to air, and leaving the a monolayer of surfactants assembled onto the substrate surface (refer to Figure 3).

The Langmuir-Blodgett technique brings to mind the relevance of the term 'adsorption' in relation to self-assembly. Adsorption describes the binding together of molecules or atoms to form a layer upon a surface; it differs to absorption in that absorption describes the passage of a liquid into or through the bulk of another medium, so that it is impossible to tell that the two sets of molecules are a different entity. However with adsorption the molecules are loosely held on top of the surface and can be distinguished. The force or bonding holding these molecules in place changes depending on the molecule. Every example of self-assembly incorporates adsorption (or a strong attraction between an appropriately functionalized head group and substrate surface) involving physisorption, chemisorption, electrostatic attraction, or covalent bond formation.[23 24 25 26]. Further examples will be shown in the following review.

2.1 Self Assembled Monolayers (SAMs)

SAMs are now an extremely important field of chemistry, with a large range of applications, more so than the Langmuir-Blodgett technique, which is more complicated and time-consuming than the spontaneous formation of SAMs. The Langmuir-Blodgett technique also restricts the level of polyfunctionality shown in more recent self-assembly techniques, which are increasingly versatile[27]. Zisman published the first real example in 1946, at which point SAMs still remained a partly unknown quality and the structural benefits of self-assembly had yet to be fully understood. Zisman, while experimenting with dilute solutions of eicosyl alcohol ($C_{20}H_{41}OH$) in *n*-hexadecane found that a drop of *n*-hexadecane wouldn't wet the surface of a pyrex flask. He concluded that the eicosyl alcohol had adsorbed onto the pyrex. He then repeated the experiment instead using platinum, again a monolayer of eicosyl acid adsorbed onto the surface[28].

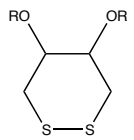 R =	Thickness of film by ellipsometry, Å	Estimated max vertical chain extension, Å	Contact angle of water/ wetting angle, degrees
$CF_3(CF_2)_6CO$	10.5±1.0	15.5, 11	104±1
$CH_3(CH_2)_{14}CO$	20.5±1.0	25	96±1
$O_2NC_6H_4CO$	9.5±2.5	12.5	52±2
CH_3CO	7.0±2.5	8	47±1
CF_3CO	4.0±0.5	9	57±1
H	5.0±0.5	6	34±1
$(HO_2C(CH_2)_2S)_2$	4.0±0.5	6	13±2
$(CH_3(CH_2)_{15}S)_2$	21.5±1.0	22	99±1

Table 1 *– Properties of disulfide solutions adsorbed onto evaporated gold films at room temperature, as reported by Nuzzo and Allara.*

Real interest in SAMs has increased significantly over the past couple of decades. Many self-assembly techniques have since been established, however monolayers of alkane-thiolates on gold are probably the most studied to date[29], these specific SAMs were recorded originally by Nuzzo and Allara. The technique they produced prepared supported, orientated monolayers of polyfunctional organic molecules with a variety of molecular structures and functional groups[30]. Organization of the disulfide films onto the gold substrate happens spontaneously. In their experiment Nuzzo and Allara covered a zerovalent gold (substrate) surface for a minute with a number of dilute disulfide solutions (~10^{-2}M) in a variety of solvents. Table 1 details the properties of different disulfide monolayers self-assembled onto the gold surface and shows that by knowing the size of the molecule assembled the thickness of the layer can be calculated.

The structures of SAMs are dependent on the substrate on which they form, unlike Langmuir-Blodgett films. This is shown in a number of examples. Trichlorosilanes (e.g OTS – *n*-octadecyltrichlorosilane) have been observed to form spontaneous monolayers onto silicon-based substrates[31 32 33], or in the case of Ratner *et al*. triiodosilanes. They are a good example of chemisorption and also demonstrate the ability of SAMs to change functionality and monolayer width. The self-assembly mechanism describes the adsorption of the trichlorosilanes through chemisorption *via* hydrolysis of the Si-Cl bonds, and the subsequent formation of Si-O-Si bonds to the substrate surface[34]. Chemisorption is stronger than physisorption and involves the formation of covalent bonds, unlike physisorption, which relies on weak Van der Waals attractions to bind to the substrate surfaces. Surfactants that physisorp to substrates are easily removed by increases in temperature and competing chemisorping molecules. The reaction scheme shown in Figure 4 describes the reaction carried out by Ratner *et al*. Also see Figure 5, which demonstrates the difference between physisorption and chemisorption.

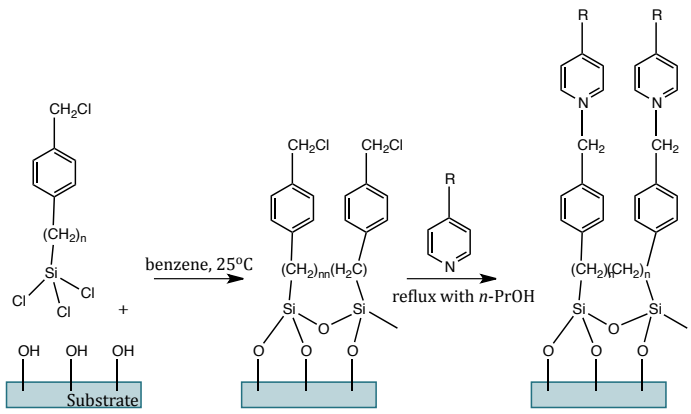

Figure 4 *– Reaction scheme of silanating of a silicon based substrate (usually glass)*

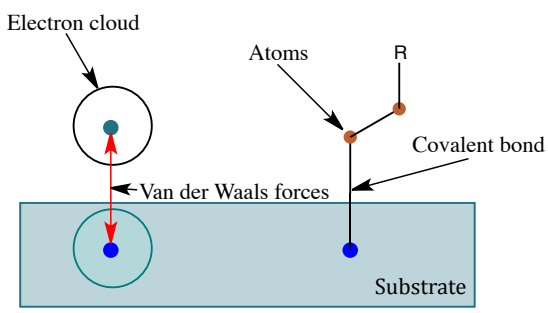

Figure 5 *– demonstrates the difference between physisoprtion (left) and chemisorption (right). The Van der Waals forces can be seen holding a molecule weakly to a substrate atom (physisorption), bond enthalphy of ~10^{-3}kJmol^{-1}. Another substrate atom actually covalently bonds to a molecule (chemisorption), bond enthalphy ~300kJmol^{-1}.*

The two main forms of synthetic self-assembly have been described in this review. Firstly the formation of alkane-thiolates on gold subtrates, binding through covalent bonds, and secondly the salination of a silicon based substrate. There are many variations to these two fundamental self-assembly techniques. However the instant formation, flexibility and simplicity of SAMs renders these techniques exceedingly useful.

In nature self-assembly is incredibly complex and difficult to re-manufacture. However the functionality of each SAM can be well observed and organized synthetically. The formation of a SAM can be monitored using electrochemical[35], optical (ellipsometry[36]) and infrared reflection absorption spectroscopy[37]. The structure of an SAM can then be viewed using an SEM (scanning electron microscope) where electrons are fired at the SAM surface, those electrons that reflect off the surface are then collected in a detector, which analyses the intensity of the electron beam along with the angle of incidence compared to the surface, a detailed image is then built up from the detection patterns, showing the surface topology.

3.0 Diamond Nanoparticles (DNPs)

It was 4000 years ago that diamond was first found in India. Diamond has since become one of the most widely known compounds in the world. From myths about diamond filled valleys guarded by snakes, to wars in Sierra Leone and miners being told of diamonds 'poisonous' properties to stop them swallowing and stealing rough diamonds. Diamonds have always been a source of huge insatiability. It was only in July 1963 that it was discovered that man could create diamond *via* detonation. Although the major source of research into 'industrial diamond' occurred in the USSR during the cold war era 1982-1993[38]. Nowadays however through the discovery of diamonds semiconducting properties, research using industrial nanodiamond is at its most intense.

3.1 Synthesis of DNPs

Natural diamond is formed over millions of years under extreme temperature and pressure. Although such conditions are problematic in a laboratory circumstance on a cost and equipment basis, diamond can still be synthetically produced.

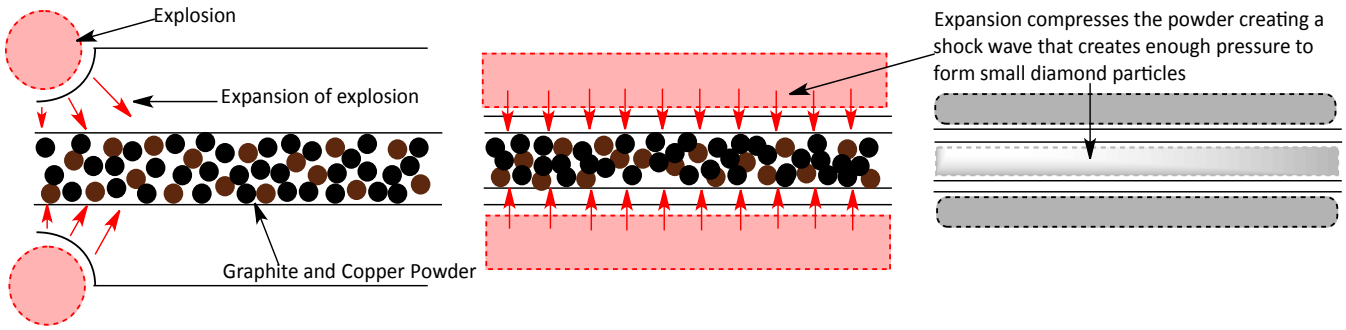

Figure 6 *– The shock-wave from the explosion creates enough pressure to force the graphite together into industrial diamond. The copper acts as a heat insulator, transferring heat more efficiently. The diamond is formed as small particles (~10nm) with a dark grey colour.*

High pressure, high temperature diamonds are formed by the compression of graphite, in the presence of group 12 metals or hydrogen as a catalyst, under conditions designed to mimic, as closely as possible, those found in the formation of natural diamond[39]. The graphite under these pressures has to form a stable octahedral structure rather than remain in a layered formation hence it rearranges to become diamond.

These conditions can be replicated using shock waves; a copper and graphite powder mixture can be dynamically shock-compacted into diamond (see Fig.6). The graphite copper powder is inserted into a tube, which is surrounded by explosives and, when exploded, increases the

pressure and temperature in the tube enough to form diamond. The copper is used to improve the heat transfer and the technique is called 'rod-in-cylinder'[40] or shock synthesized diamond[41].

Detonation is another way of creating industrial diamond. This method uses graphite as the explosive mixture itself alongside TNT and hexagon. As the detonation wave passes through the reactor it compresses the graphite mixture into diamond[42 43], regularly producing DNPs ~10nm.

The final method of creating diamond without having to use large pressures and temperatures is CVD (Critical Vapour Deposition). Gases are energized, including a carbon containing gas and the conditions are then adapted for the gas to break down and start to grow sp^3 hybridized carbon atoms onto a substrate surface. This method arranges atoms in thin films[44]. The two main types of CVD are hot-filament (HFCVD) and microwave plasma (MWCVD)[45]. CVD diamond is usually less functionalised than self-assembled diamond and most examples are grown on silicon substrates rather than the metal substrates used in this review. CVD diamond is a relatively complicated process in comparison to self-assembled diamond, and less commercially accessible and although CVD diamond particles are conventionally of the size ~80-100nm they are grown as thin films not monolayers and therefore do not display as many nanofacets as self-assembled diamond. Due to the reasons above the barrier for thermionic emission of CVD diamond is likely to be higher than that found of self-assembled diamond.

3.2 Properties of Diamond Nanoparticles

Diamond nanoparticles have a number of unique and important characteristics, which give rise to the large number of applications. Diamond as a material is incredibly stable due to strong covalently bonded sp^3 hybridised carbon in a giant diamond cubic lattice; diamond is the hardest known material and has the highest thermal conductivity of any element at room temperature, as well as a very low thermal expansion coefficient. Diamond is an electrical insulator and can withstand incredibly high electric fields[46 47]. DNPs are incredibly useful within the electronic industry[48], because it can be doped with elements such as boron, turning it into a semi-conductor. This has led to DNPs being assembled onto electrodes, to further the number of electronic applications it can be used for (topic expanded later in section 4.2).

DNPs have a small average particle size and come in a narrow range of particle sizes. With facile surface functionalization and high biocompatibility[49], DNPs can be used for many biological applications including drug delivery and biomarkers.

3.3 P-type and N-type Doping of Diamond Nanoparticles

Doping of diamond is essential for electronic applications due to diamond's insulating properties when un-doped; diamond has a wide band gap (E_g = 5.5eV). Boron is usually used as a doping agent due to its similar atomic radius to carbon; as diamond has a densely packed lattice, boron is relatively easily incorporated. Boron when doped onto the DNPs gives rise to additional electronic levels in the diamond band gap[50] to just above the valence band reducing the band gap (E_a=0.37eV). Boron acts as an electron acceptor and induces a p-type state in the band gap of diamond, these extra electronic levels or states in the band gap, created by doping with boron, of diamond act to make boron doped diamond a semiconductor as when electrons are thermally excited deficiencies of valence electrons in substituted atoms generate holes in the valence band that can hop from one site to another which act as mobile charge carriers[51 52], this is the basis for thermionic energy emission, an important potential application[53 54]. When doped with 10^8 boron atoms per cm^3 the resistivity of the semiconducting diamond is $10^4 \Omega$ cm. By increasing the dopant to 10^{20} boron atoms per cm^3 the resistivity drops to 10^{-3} Ω cm, therefore indicating semi-metal type character[55]. A semiconductor such as this that is incredibly stable under harsh conditions is extremely useful in electrochemistry and has many further applications.

N-type doping of diamond is also possible. This is almost the opposite of p-type donating in that both techniques involve the addition of extra electronic states or levels within the large insulating band gap of diamond. However where p-type doping produces an electron-accepting band just above the valence band, n-type doping involves donor atoms that induce an additional band close to the conductance band. Thermal excitation of electrons from this additional band to the conductance band renders these electrons 'free'[56], meaning they're free to carry charge, which classifies n-type doped diamond also as a semiconductor.

N-type doping is still relatively un-tested in comparison to p-type, which has been tried and tested. Group one metals can be used for n-type doping; in this review the nanodiamonds are prepared by doping with lithium before the self-assembly process. Lithium can be doped into diamond via ion implantation[57], although this technique is still very experimental. Li is found to be an interstitial donor with an energy level E_c= -0.1eV[58]. This should give rise to highly desirable shallow donor levels in the diamond. *T. L. Martin, et al. (2011)*[59] observed, using x-ray photoemission spectroscopy, a thin layer of lithium on oxygenated boron-doped diamond. Lithium was evaporated onto the oxygen-terminated surface and formed a strong lithium-oxygen bond.

Doping of diamond is not the only method to turn insulating diamond particles into semi-conductors. The surfaces of DNPs can be terminated or functionalized. Hydrogen plasma treatment terminates the surface of DNPs with hydrogen atoms, whilst halide functionalization, alkylation, and amination functionalize surface diamond particles with groups such as ketones, or carboxylic acids[60]. DNPs can also be oxygen terminated; O-termination opens up a wide range of further chemical functionalisation with an exciting range of applications. Functional groups play a vital role in chemical behavior, for example H-terminated diamond is much more hydrophobic than O-terminated diamond[61].

3.4 Surface Termination of DNPs

Modification of a diamond surface and its conductivity depends largely on whether the surface of the diamond is terminal or passivating[62], as these characteristics have a large impact on the electron affinity of the surface. Electron affinity describes the difference in energy of the conduction band and vacuum level. Negative electron affinity is needed to create the desired electronic properties. As negative electron affinity causes the conduction band lie above the vacuum level, allowing electrons to be high enough in energy to emit from the surface[63]. Funtionalisation of diamond surfaces produces surface dipoles due the electron donating or withdrawing properties of the groups added. In order to achieve negative electron affinity, electron density must decrease away from the surface. This creates a potential drop across the dipole that causes band bending and the conductance band moves closer to the surface, meaning it lies above the vacuum level[64].

Hydrogen terminated diamond surfaces display a strong negative electron affinity in the range of ~ -1.3eV[65]. The most common practice of terminating diamond with hydrogen is H_2 plasma treatment at 870^0C and H_2 gas at ~40mbar[66 67]. However, CVD grown diamond is usually terminated with H_2 on formation[68], which has lead to increased interest in this field. Hydrogen terminated surfaces do not have a set structure, although singly bonded hydrogen (monohydride) attached to each carbon individually is the most common.

Hydrogenation produces a decrease in resistivity due to increased hole conduction, leading to an increase in the p-type character of the diamond surface[69]. Hydrogenation can lead to diamond undergoing the surface transfer doping mechanism, where ions on the surface act as acceptor ions and remove electrons from the valence bands, creating holes that are localized to the surface[70 71]. This highly conducting property has major implications on further electronic applications.

H-terminated diamond surfaces have been proved to show thermionic emission properties with stability of up to 745^{0}C, as hydrogen desorbs above this temperature.

Oxygen terminated diamond surfaces display positive electron affinity (PEA) around ~ 1.7eV[72], and can be useful in generating negative electron affinity in surfaces. PEA of O-terminated diamond surfaces is caused by the dipole formed at the oxygen carbon surface bond; as oxygen is the more electronegative element, the electrons in the bond are drawn towards the oxygen atom and away from the carbon (diamond) surface, causing downward band bending, and leaving a positive electron affinity. One method of obtaining oxygenated diamond is the thermal oxidation which is carried out in a controlled furnace at ~600^{0}C with air as the source of oxygen. Another method of terminating diamond surfaces with oxygen is acid treatment with a 9:1 nitric: hydrochloric acid bath.

The most important observation of surface modification is the electronic properties these techniques induce onto diamond, usually insulating, creating a self-conducting species through changes in charge density and surface electronic properties[73 74 75].

The properties, derived above, of modified DNPs make them extremely useful in electronic applications. Hence there is an emerging field involving the self-assembly of semi-conducting DNPs onto substrates for use in electronic devices. Section 4.2 describes the applications of these modified DNPs and how their range of applications is greatly increased by their ability to semi-conduct.

4.0 Self-Assembled Diamond Monolayers

Many self-assembly techniques have been researched throughout the years, focusing mostly on the self-assembled monolayers of alkane thiolates on gold substrates and salination of silicon based substrates; as shown in section 2. However, emphasis has recently turned to the application of small diamond nanoparticles (DNPs) onto substrate surfaces through self-assembly. The increase in interest towards this particular SAM is generated by the high chemical stability and the ability to terminate or dope the diamond surfaces with different functional groups which means that DNPs can be used for a huge range of applications including biomarkers, thermal electron emitters, single photon sources, drug delivery, high performance nano electro-mechanical systems, amongst many other purposes[76 77 78].

4.1 Applications of DNPs

Diamond is biocompatible due to its foundation from a carbon lattice, and has three main uses in biology: the immobilization of proteins for separation or purification, a delivery agent to introduce biological moieties into cells, and as a fluorescent marker for cell imaging[79].

Bonder *et al.* demonstrated an example of DNPs being used to separate proteins in 2004. DNPs show unique physiochemical properties, with a highly developed surface of particles (270-280 m^2/g)[80], and a large degree of surface functionalization. Proteins were separated from *Escherichia coli*, once the cells were broken down (*via* ultrasound) and the debris removed (*via* centrifugation) the proteins in solution were physisorbed onto DNPs and the rest of the sediment was removed leaving only the proteins adsorbed onto the DNPs which were then desorbed to leave a pure protein solution.

DNPs are also used in drug delivery, they are biocompatible, can target specific areas in the body and therefore reduce drug release at unaffected sites, minimizing unwanted side affects and other complications[81]. Huang *et al.*[82] used DNPs as chemotherapeutic drug carriers. Doxorubicin Hydrochloride (DOX), an apoptosis-inducing drug was amalgamated to DNPs. DOX terminated DNPs were found to move quickly and freely within the cells around the body. The interaction between the DNPs and DOX is helped by the functionalization of the diamond surface with a carboxylic acid (COOH) group leaving negatively charged (COO^-) DNPs to interact with the cationic DOX ions ($D\text{-}NH_3^+$). However NaCl is needed to improve the loading process and aid adsorption; Huang *et al.* reported that without NaCl less than 0.5wt% of DOX would adsorb onto the DNPs, while NaCl 10wt% would adsorb. DOX can be released from the nanodiamond *via*

desalination, for example. Although there are a number of more targeted methods for releasing the drug, by tailoring the functionalization of the DNP surface with antibodies for example, DNPs would release the proteins at specific locations in the body due to the break down of the protein-nanodiamond aggregate in specific conditions[83 84]. Further examples of DNPs used in drug delivery can be seen where DNPs are coated with polymers to attract covalent attachment of

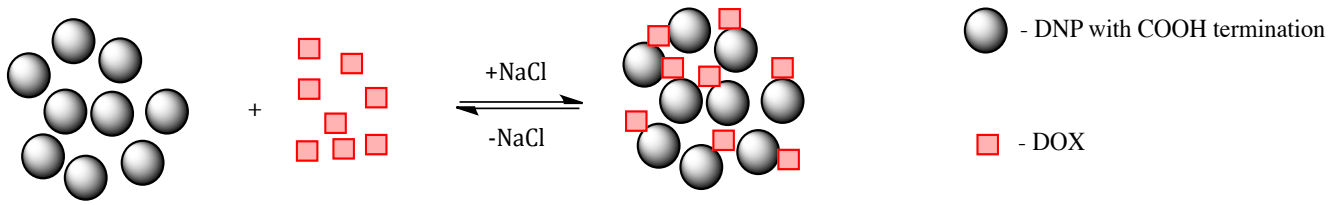

Figure 7 *– Shows a simplistic mechanism for the drug delivery reaction described by Huang et al (2007). Where DOX protiens are adsorbed on DNP surfaces and then desorbed in the affected area of the human body.*

proteins, for release at targeted sites in the body[85].

Puzyr *et al.* showed that the adsorption of enzymes and antibodies onto DNPs can lead to important sensory devices. The enzymes did not lose their catalytic ability and hence a luminescent biochip was created for bioluminescent analysis[86].

Fluorescent cell imaging is made possible by negative nitrogen vacancy centers within the DNPs[87], induced by high-energy ion beam irradiation and subsequent thermal annealing, resulting in a strong fluorescence at 700nm and absorbance around wavelengths of 560nm. A good biomarker should emit light above 600nm to deeply penetrate through cells and tissues[88]. The surface of the DNPs can be modified without any change to the fluorescence, which lasts for an impressive 300s (compared to the 10s produced by a dye molecule); this intensity is similar to the found in quantum dots, however, DNPs are non-toxic[89]. Fu *et al (2007)* proved experimentally that 100nm diamond was taken up by and formed aggregates within the cytoplasm of cells in human kidneys. This was confirmed using fluorescence microscopy[90].

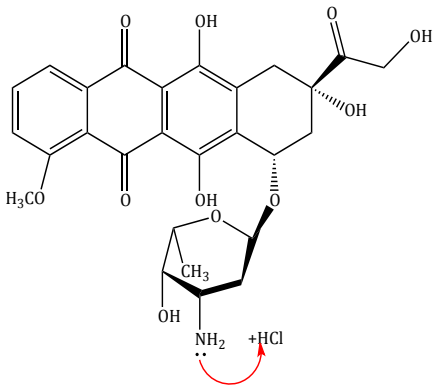

Figure 8 *– The Doxorubicin Hydrochloride (DOX) molecule corresponding to Fig. 7.*

DNPs have a few interesting mechanical properties too. Due to their incredible resilience and hardness, they can be applied to power cutting tools in reduce the wear of the metal and improve their efficiency, or in the polishing of materials such as watch sapphires, hard disks, etc[91].

These applications rely on non-conducting diamond particles. By inducing electronic behavior into DNPs via surface modification, as described in sections 3.3 and 3.4, conductivity can be stimulated within DPs greatly increasing the applications available.

4.2 Conducting DNPs and their applications

The applications based on conducting DNPs are possibly the most exciting. 'Diamond is expected to be one of the most suitable materials for high-power, high-frequency electronic devices due to its high electronic break down field (>10MV cm^{-1}), high carrier mobility (4500 cm^2 V^{-1} s^{-1} for electrons, 3800 cm^2 V^{-1} s^{-1} for holes), high thermal conductivity (22 W cm^{-1} K^{-1}), and high saturation velocity (1.5×10^7 cm s^{-1} for electrons, 1.05×10^7cm s^{-1} for holes)'[92].

However, there are still problems to overcome in order to use diamond in electrical devices. Thin films of diamond are polycrystalline and contain many defects that reduce the effective mobile charge carriers[93]. Another issue is that in order to replicate the features of microcircuitry, diamond needs to be self-assembled in a very specific manner onto the substrate. Nonetheless there are key techniques known to achieve this nano assembly. Diamond can be etched into O_2 plasmas, and (Chalker and Johnston, *1996*[94]) produced a technique called selective area deposition (SAD)[95]. The final issue is in accordance to doping DNPs, n-type doping is difficult due to diamonds structural rigidity making it very hard to dope the diamond with any atom larger than carbon; Only recently have papers deciphering viable techniques been released. Since then electronic systems using thin diamond films have started to appear, especially in systems open to harsh temperatures or conditions.

4.2.1 Electronic Applications

Semiconducting field-effect transistors (FETs) are well-studied electronic applications involving conducting DNPs. FETs use electric fields to control and channel the conductivity of charge carriers in semiconducting materials. *Ishizaka et al. (2003)* [96] demonstrated the construction of FETs configured as shown in Fig. 9, using semi-conducting DNP thin films.

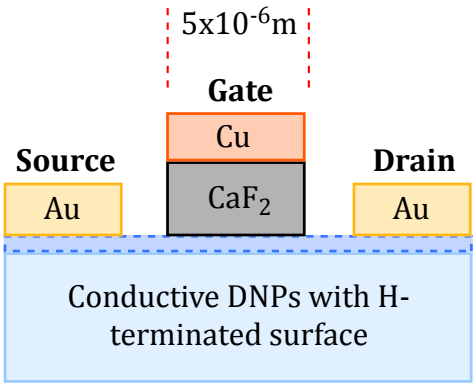

Figure 9 *displays the FET described by Isizaka et al.*

DNPs have been used for high performance nanoelectromechanical systems (NEMS)[97]. These systems link the electronic functionality of transistors and adapt them for use with mechanical devices such as pumps, forming useful biological or chemical sensors at a

nano scale. S. Mandal *et al. (2010)*[98] grew super conducting (highly boron doped) diamond onto silicon oxide substrates *via* microwave plasma chemical vapour deposition (MPCVD). The thin diamond films are patterned into nanostructures using a standard electron-gun evaporator, a thin nickel film (65nm) and the 'lift-off' technique. Using this electron-beam lithography Mandal *et al.* were able to process NEMS of less than 100nm.

Diamond Superconducting Quantum Interference Devices (SQUIDs) are used to measure extremely weak changes in magnetics fields. Micrometer SQUIDs have been discovered by *S.* Mandal *et al. (2011)*[99] with the use of superconducting DNPs made by highly doping diamond with boron above the critical level (~0.25atom %). These SQUIDs were demonstrated to work in magnetic fields of over 4 Tesla (rather than 1T previously). This is a decisive step towards the detection of quantum motion in a diamond based nanomechanical oscillator.

Characteristics:		Bare Molybdenum	Single DNP	DNP Film
Geometrical:	Metal tip radius	50nm	50nm	50nm
	ND thickness	0nm	2.3nm	20nm
Field Emission:	Threshold conductance	172V	222V	89V
	Trans conductance	7.63nA/V	7.09nA/V	16.40nA/V
Analysis:	Work function	4.05eV	5.57eV	2.71eV

Table 2 – *Produced by Tyler et al. after experiments to determine the emission properties of polycrystalline diamond films assembled on FEDs.*

"Polycrystalline diamond films have been observed to emit electrons with intensity sufficient to be imaged in the accelerating field of an emission microscope without external excitation[100]". This gives them vital properties used in Field Emission Devices (FEDs) and flat panel displays[101]. Tyler *et al. (2003)*[102] noted the interesting field emission properties of DNPs when self assembled onto molybdenum needles. For a number of years it had been thought that coating metal FEDs with diamond would seriously improve their cold emission of electrons, however the field was not fully understood. By self-assembling diamond thin films onto a needle shape emitter Tyler *et al.* discovered, through a number of experiments, that single particle layers of diamond (monoloayers), with a film thickness ~2nm, emitted electrons most successfully. Where as if the diamond film was >20nm the emission properties were lower than that of the bare metal. Table 2; shows the results produced by Tyler *et al.*

Thermionic emission is another possible use of DNPs and potentially one of the most important, due to the growing demand for a reliable and efficient energy source. Thermionic energy converters work with an electrode at an extremely high temperature, diamond has been found to

be a good semi-conductor to coat these electrodes with. Section 5 further explains the use of DNPs in thermionic energy converters.

Semiconducting diamond has the potential to be used in quantum computing.

4.2.2 Catalytic Applications

Conducting diamond can be used as a catalyst supporting material in electrocatalysis to take advantage of its electrochemical stability and the ability to easily modify the surface of DNPs. DNPs are self-assembled onto electrodes and support the metal catalysts to insure they don't deteriorate at high temperatures. This process has been put to most use in fuel cells. Boron doped diamond is modified with metallic oxide catalysts and assembled onto electrodes, leaving high area and very stable electrodes. Methanol oxidation is used in fuel cells due to its high energy density (Wh mL^{-1})[103]. Pt and Ru are very good electrocatalysts however they when being used in methanol oxidation they often get poisoned by intermediates such as CO[104]. Boron doped nanoparticles were used to support Pt-RuO_x catalysts by Salazar-Banda *et al. (2007)*[105] to overcome problems such as the poisoning and break down of the catalysts. The boron doped diamond electrodes possessed a wide electrochemical window and a low background current. They noted that the boron doped diamond and Pt-RuO_x electrodes had a brilliant activity for methanol oxidation presenting and onset potential 20mV lower than the potential recorded for a commercial Pt-Ru and carbon catalyst.

4.3 Self-assembly of DNPs to Electrodes and Corresponding Analytical Applications

As explained in this review diamond is readily applied to electrodes for electrochemical applications. The examples shown thus far include electrocatalysis and thermionic energy emission. The effect of coating electrodes with diamond has many positive affects on the performance of diamond none more so than the fact that self-assembling diamond onto an electrode increases the surface area of the electrode and, therefore, increases the area available for collisions or emission of electrons a phenomenon not yet discussed in this review.

Semi-conducting diamond coated electrodes can also be used in a number of detectors. Zhao *et al. (2006)*[106] assembled a thin nanodiamond film onto an amide modified gold electrode for the selective detection of glucose (electrochemical glucose sensor). Glucose oxidase bonded to the DNPs *via* amide linkages. The modified electrode promoted the electron transfer rate within the nanodiamond surface, but it also increased the reduction of the dissolved oxygen, from this

information levels of glucose were monitored at negative potential by censoring current change in the rate of the reduction of oxygen. Diamond coated electrodes have also been used to detect a number of metal ions, and other biological compounds[107].

Other notable papers describe further interesting applications of diamond. In his Diamond thin films P. May *(2000)* describes a number of applications for CVD diamond. It is again noted how the range of applications is greatly increased by the adaptation of semi-conducting diamond. Professor Gehard Materlik has been working on diamond as a source of synchrotron light[108].

5.0 Thermionic Energy Conversion

It is well documented that the world's energy demand is high. Exxon Mobil, in a recent survey, predicted that by 2030 global electricity demand would be 30,000 TWh per day, 50% more than todays demand, driven by the increasing demand in developing countries. Finding a source for renewable energy is paramount as fossil fuels are in major decline and hence current methods of energy generation are not viable on a long term. The UK is undergoing a large change to Nuclear. Which might reset the balance and improve on the current 3.4kHh per day per person produced by nuclear in the UK.

Thermionic energy conversion is a method of converting heat to electrical energy. Electrons from an extremely hot cathode are emitted through vacuum onto a cold counter electrode, a self-generated voltage (<1V) then appears across the gap (~500μm). An electrical current can then be established by connection of the two electrodes[109 110]. Richardson and Dushman first documented the origins and theory of thermionic emission with the expression[111 112]:

$$\boldsymbol{J(T) = AT^2 e^{-\varphi/k_{BT}}}$$

Where: J = Emission current density (A cm^{-2})

A = Richardson constant (A cm^{-2} K^2)

φ = Work function (eV)

T = Temperature (K)

K_B = Boltzmann constant (m^2 kg s^{-1} K^{-1})

It has been found that the NEA of hydrogen terminated diamond surfaces reduces the emission barrier. Thermionic energy converters (TECs) with cathodes made from metallic composites and oxides often operate successfully at 1000^0C with a work function of 2eV[113]. *F. A. M. Koeck et al. (2011)*[114] concluded that phosphorus and nitrogen doped diamond layers on metallic substrate cathodes thermionically emitted at 500^0C when exposed to methane with work functions of 1.18eV and 1.44eV respectively, showing a huge increase in efficiency.

This is down to the process of extracting electrons from the conduction band to the vacuum level, the barrier of which defines electron affinity and contributes towards the overall work function of the material. By reducing the barrier of emission the work function is lowered and therefore eases the transition or emission of electrons from the conduction band to the vacuum band.

Semiconducting diamond has a negative electron affinity as explained in section 3.3 of this review. Most semi-conductors have positive surface electron affinity, which holds the electrons tightly to the surface of the conduction band, making emission more difficult.

Many research groups have been trying to harness the potential of thermionic energy conversion that could be a very lucrative breakthrough in technology; such is the demand for more efficient energy sources. TECs could be deployed within nuclear and coal fired power stations to improve efficiency by harnessing 'waste heat' and converting it to electrical energy.

Thermionic emission using diamond nanoparticles has been attempted as a side to this review. The barriers to emission are still too high to be considered commercially viable. The layer of self-assembled diamond needs to be even use diamond of <350nm ideally, to create the number of nano-facets needed to lower the barrier of emission.

Thermionic emission through excitation with Beta particles is also being studied.

6.0 Electrochemistry of Diamond

Electrochemical studies into conducting diamond films were first published by *Y. V. Pleskov et al. (1987)*[115]. The paper detailed the assembly of conducting diamond thin films onto electrodes. It concluded that conducting diamond particles could be grown onto a substrate via CVD or other self-assembly techniques (discussed in this review) and that diamond electrodes possess excellent electrochemical properties such as a wide electrochemical window, low background current, and high corrosion stability[116 117 118].

Electrochemical properties of DNPs are measured by the heterogeneous rate constant (k_{et}). However, as evaluated in this review, DNPs need to have undergone some form of surface modification in order to become semi-conducting. Boron doped diamond (BDD) is the most widely used diamond particle in electrochemistry. Using BDD, the value of k_{et} is subject to changes in doping levels, film qualities, electrode surface terminations, and types of redox probes or species[119]. These types of redox species are characterised into surface insensitive groups and surface sensitive groups.

Surface insensitive groups (e.g. $Ru(NH)_3^{3+/2+}$) as the description suggests show insensitive electrochemical responses to electrode surfaces (BDD). The k_{et} values displayed by these groups upon BDD electrodes are very similar to those indicated by glassy carbon electrodes, around 0.01-0.2 cm s^{-1}, which is high enough to use as electrode material[120].

Surface sensitive groups such as $Fe^{2+/3+}$ show electrochemical responses that, due to their increased sensitivity, are also affected by oxide formation, surface adsorbed species, surface impurities, surface functionalisation, and grain boundaries[121]. Surface sensitive species such as these are widely used due to their low k_{et} values. $Fe^{2+/3+}$ has k_{et} values of 10^{-5} cm s^{-1} showing a very slow electron transfer at the H-terminated BDD electrode, due to the lack of adsorption sites on the electrode[122].

It is also possible to look at the electrochemical properties of DNPs separately rather than just thin films of boron doped diamond nanoparticles. There are fewer studies in this vain however leaving boron doped thin diamond films the most widely used electrochemical diamond compounds.

7.0 Experimental Techniques

MSY005 grade High Temperature High Pressure (HPHT) diamond was purchased from Microdiamant AG, Switzerland, nominal size 500nm and acid washed. Acid treatment was initiated in a concentrated acid solution (9:1 Nitric : Sulphuric acid), heated gently for ~4hrs, and separated; for use in self-assembly and electrochemical analysis.

7.1 Self-Assembly

Self-assembly as mentioned earlier is an important part of this review. Diamond nanoparticles were self-assembled onto Tungsten, ITO (Indium Tin Oxide) covered glass and Tantalum substrates in order to form electrodes for thermionic energy emission.

Trial and error was used as a technique to analyse the optimum conditions for self-assembly of DNPs onto substrate surfaces. The metal substrates were washed in KOH (40wt%) for ~30mins, rinsing with deionised water and transferring the substrates to a 0.1-1wt% solution of deionised water and PEI polymer (poly-ethyl-imine) for either ~30secs or ~30mins. Proceeded by rinsing with DI water, drying under a stream of argon, and then pipetting ~1wt% (pH 7.5-8.5) diamond solution onto the substrates for ~1hr. The substrates were then rinsed and dried using DI water and argon. Analysis of the diamond assembled on the substrates *via* SEM and optical microscope was then undertaken.

ITO substrates were successively washed for 10mins, whilst sonicating, in acetone, ethanol, and finally in DI water, before immersing in the polymer solution.

The Diamond solutions were made by suspending the HPHT diamond nanoparticles in DI water to the correct weight percentage and adjusting the pH with NaOH and then sonicating.

Samples were often vacuum annealed to preserve the DNPs on the substrate.

7.2 Optical (Nomarski) Microscopy Technique

This technique was used to analyse the surface morphology and estimate surface nanoparticle coverage.

The Nomarski microscope is often used to image samples of poor optical parity, via bright field illumination. Micro-topographic differences that typical optical microscopes wouldn't observe can be viewed using the Nomarski microscope, along with better resolution of microtextures. This effect is possible due to polarizing lenses within the microscope

Once samples had been prepared, this optical microscope was used to observe the surface coverage of nanoparticle on the substrate.

7.3 Scanning Electron Microscopy (SEM)

The SEM was used as a further confirmation of surface diamond coverage, as well as to observe the size of particles assembled onto the substrate.

SEM develops high-resolution images of surfaces on the nanometer scale. The image is produced by a primary beam of electrons emitted from an electron gun, which scans over the surface of the sample causing electrons and x-rays to emit from the sample, these are collected by detectors and secondary detectors which then convert them into a visible image.

Sample electrodes, if deemed suitable enough under the optical microscope, were analysed using the SEM to further confirm their eligibility for thermionic testing.

7.4 Cyclic Voltammetry

Cyclic voltammetry and Chronoamperometry can be used to electrochemically oxygen terminate of hydrogenate the surfaces of CVD grown nanodiamond. However within the authors' knowledge they have not been applied to self-assembled nanodiamond.

Cyclic voltammograms were run at oxygenating and reducing potentials using an Ivium Technologies CompactStat potentiostat. Self-assembled diamond on ITO substrates, or plain ITO, were used as working electrodes, with platinum used as a counter electrode (see image 1). A reference electrode was not used. For oxygenation the electrochemical cell contained a solution of 25ml of 1M sulfuric acid and 25ml 0.5M nitric acid[123], and was run through a cyclic range of potentials from 0V to 5V. For hydrogenation the cell consisted of a 2M solution of sulfuric acid; it was subjected to potentials in the range of 0V to -5V[124].

Image 1 *– Displays the potentiostat and cell used described in section 7.4.*

8.0 Results & Discussions

8.1 Self-Assembly Analysis

Self-assembly was conducted at a range of pH, diamond solution concentrations, and polymer solution concentrations. Experimental section 7.1 showed a technique that gave a good surface coverage on all the substrates.

It was known that the conc. KOH removed oxide layers from the metal substrates. PEI polymer is a well-known cationic polymer and induces a positive surface charge on the metal substrate. By making the diamond solution mildly alkaline diamonds are induced by charge to bond with the surface of the substrate.

The main aim of this review was to assess and perfect the self-assembly technique of diamond nanoparticles onto various substrates. Self-assembly is used to assure only a monolayer is formed, in order to achieve as many nano-facets as possible. It is also a commercially viable technique that could be used on an industrial scale if thermionic emission through diamond electrodes becomes a major source of energy.

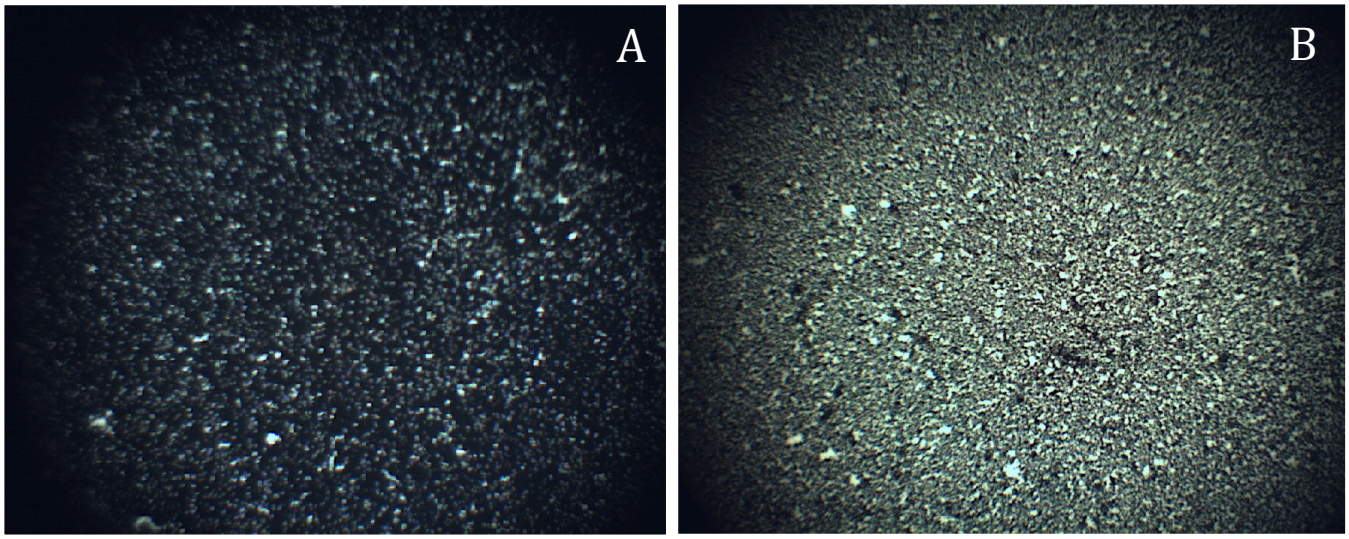

Figure 10 – *Optical Microscope images of Acid treated, Lithiated MSY Bac 441 HPHT diamond nanoparticles assembled onto Tungsten substrates. 10x Zoom.*

The electrodes produced, shown in Fig. 10A, were self-assembled with a 1wt% diamond solution of pH 8.5, as at this pH the DNPs are less likely to cluster together. The substrates were submerged in the polymer solution for 30minutes in order to induce a positive surface charge. This technique gave a good initial coverage of 60%. The weight percentage of the diamond solution was increased to 5wt% (Fig. 10B) giving a better surface coverage (80%) of diamond onto the substrate, making these electrodes acceptable in testing for thermionic emission.

Supplementary samples were run without substrates being in contact with the PEI polymer solution. Further to those, sample electrodes were also made with submergence in the polymer solution for only 30seconds.

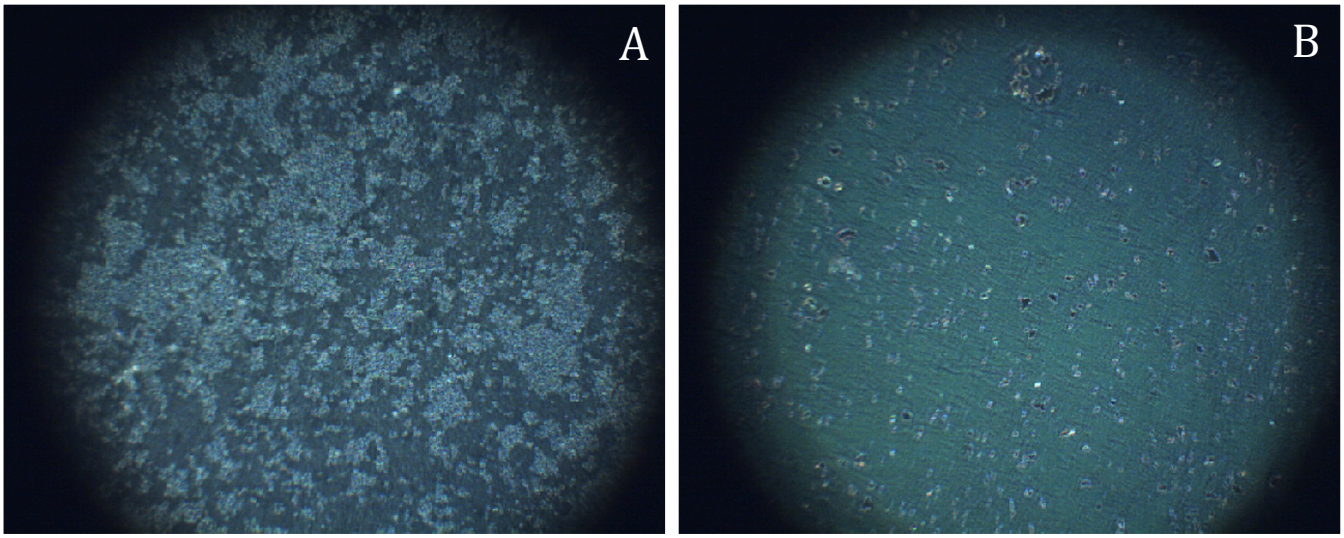

Figure 11 – *Optical Microscope images of Acid treated, Lithiated MSY Bac 441 HPHT diamond nanoparticles assembled onto Tantalum and Tungsten substrates respectively, with changes in PEI application. 50x Zoom. Both samples in Fig. 11 were hydrogen oxygen annealed.*

With limited application of PEI (30secs) Fig. 11A clearly shows a poorer surface coverage than in Fig. 10. However there is still ~50% surface, which shows there is 30% difference in coverage from leaving the substrates in cationic polymer solution in order to induce a strong surface positive dipole to attract the diamond to physisorb onto the surface of the substrate. In Fig. 11B, where no PEI was applied to the substrate, very poor coverage is observed (10%); indicating the importance of the polymer in the self-assembly technique.

When changing the pH of the diamond solutions closer to neutral (pH 7.5) DNPs appeared to cluster together, although an increase in surface coverage was observed. The optical microscope images (Fig. 12) suggest that there is possibly more than a monolayer and the clustering was not just two-dimensional, a situation possible by the high weight percent of the diamond solution. AFM could be run to determine the thickness of the diamond layer; if the layer was found to be greatly in excess of 500nm then it could be concluded that this technique was producing a series of monolayers and the lower pH had a detrimental effect on the performance of the electrodes.

Acid washed nanodiamond was compared against unwashed nanodiamond. Acid treated DNPs assembled with a much more even and higher coverage than the untreated nanodiamond. The acid treatment is known to oxygenate the diamond particles, the difference in electronegativity

between oxygen and carbon forming a permanent dipole on the surface of the acid washed nanodiamond, which could account for the improved self-assembly.

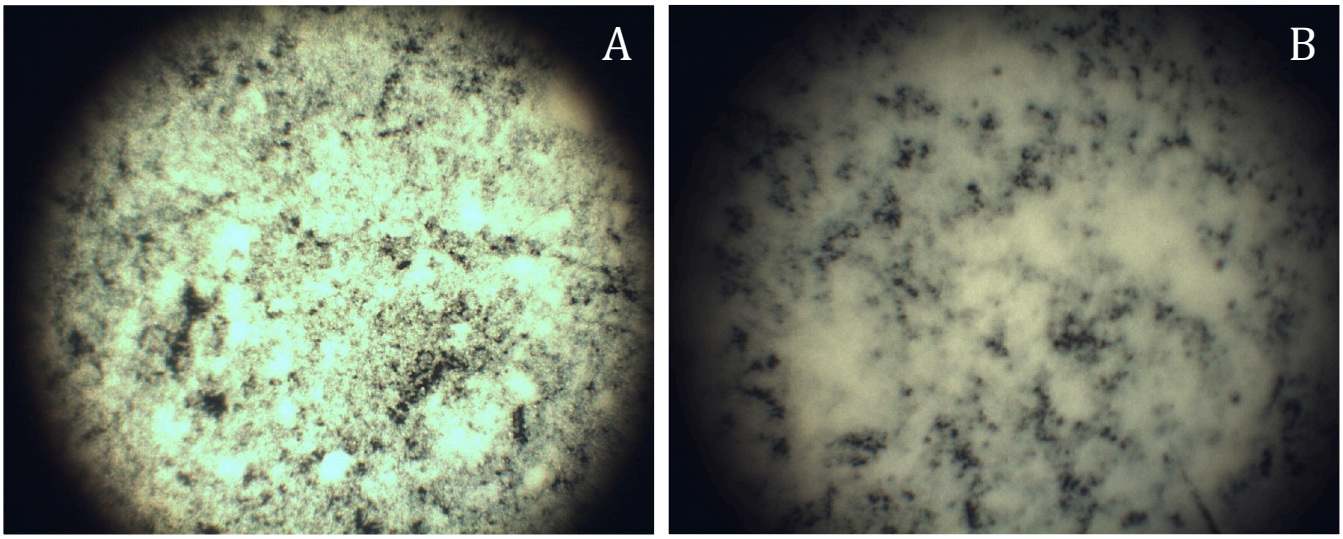

Figure 12 *– Optical Microscope images of Acid treated, Lithiated MSY Bac 441 HPHT diamond nanoparticles assembled onto Tungsten substrates, pH 7.5. 50x(A) and 100x(B) Zoom. Clumping and poor single diamond definition.*

The trend behind the self-assembly technique also varied hugely on the deposition time of the substrate with the nanodiamond: the longer the deposition times the higher percentage surface coverage, but there was also a positive correlation with the increased clumping.

Tungsten and Tantalum were used as substrates due to their high thermal stability. To the authors' knowledge the self-assembly of diamond onto tungsten and tantalum has yet to be covered outside of this research group.

8.2 Particle Size Definition

Having established the technique required to obtain an even >80% surface coverage of diamond onto metal substrates, the second aim was to get an even coverage with particles of around 200-300nm. This was necessary due to the difficulty in obtaining thermionic emission through the semi-conducting diamond layer. Therefore it was concluded that smaller particles were required to lower the barrier for emission.

Initially a centrifuge was established to be the desired method of extracting the smaller particles from the diamond solution. However the centrifuge available to the group separated all of the nanoparticles out of suspension.

A 450nm filter was unearthed and the diamond solution diluted to 0.5wt%. The solution was then pipetted through the filter and the corresponding clear solution was assembled onto the metal substrates.

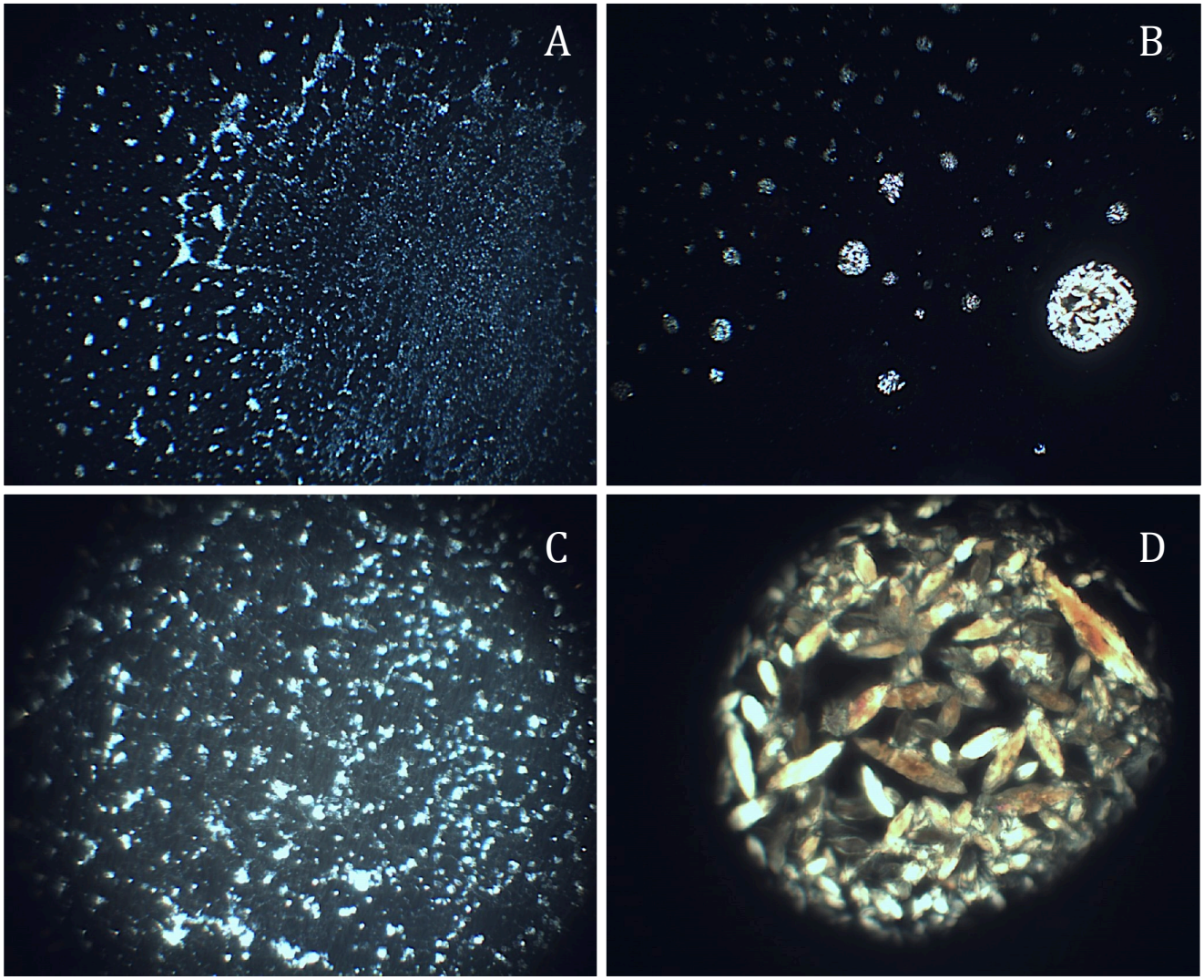

Figure 13 – *Optical Microscope images of Acid treated, Lithiated MSY Bac 441 HPHT <450nm diamond particles assembled onto Tungsten substrates, pH 7.5. 10x(A,B) and 50x(C,D) Zoom. Poor percentage coverage and diamond aggregation can be observed.*

The results (Fig. 13) showed that the filter must have blocked and liberated very few diamond particles (~0.05wt% diamond solution), hence the poor coverage. Fig.13A displays smaller particle size than previous samples. However this advantage is offset by the lack of diamond coverage and the micelle like clumping of diamond (Fig.13B). This clumping is possibly an outcome of smaller nanodiamonds being more susceptible to the cationic forces induced by the PEI polymer. It is also conceivable that the smaller oxygenated nanoparticles form temporary dipoles from oxygenated surfaces and un-oxygenated carbon surfaces, hence the aggregation of the nanoparticles occurs in the diamond solution. The micellular formations could also be a product of organic contamination from the 450nm filter.

As the filter was not entirely successful and so the filter process was reversed. By pipetting DI water backwards through the blocked diamond filled filter the smaller nanoparticles were the first liberated; 20ml of DI water was passed back through the filter, forming a cloudy solution (~2wt%). The solution was then sonicated for 15mins, and allowed to rest for 5mins. After 5mins the top fraction (10ml) was separated, forming a new solution and isolating the smaller diamond particles. This solution was adjusted to pH 7.5. At this pH it was deemed that better surface coverage was achieved at the expense of the formation of some minor aggregation.

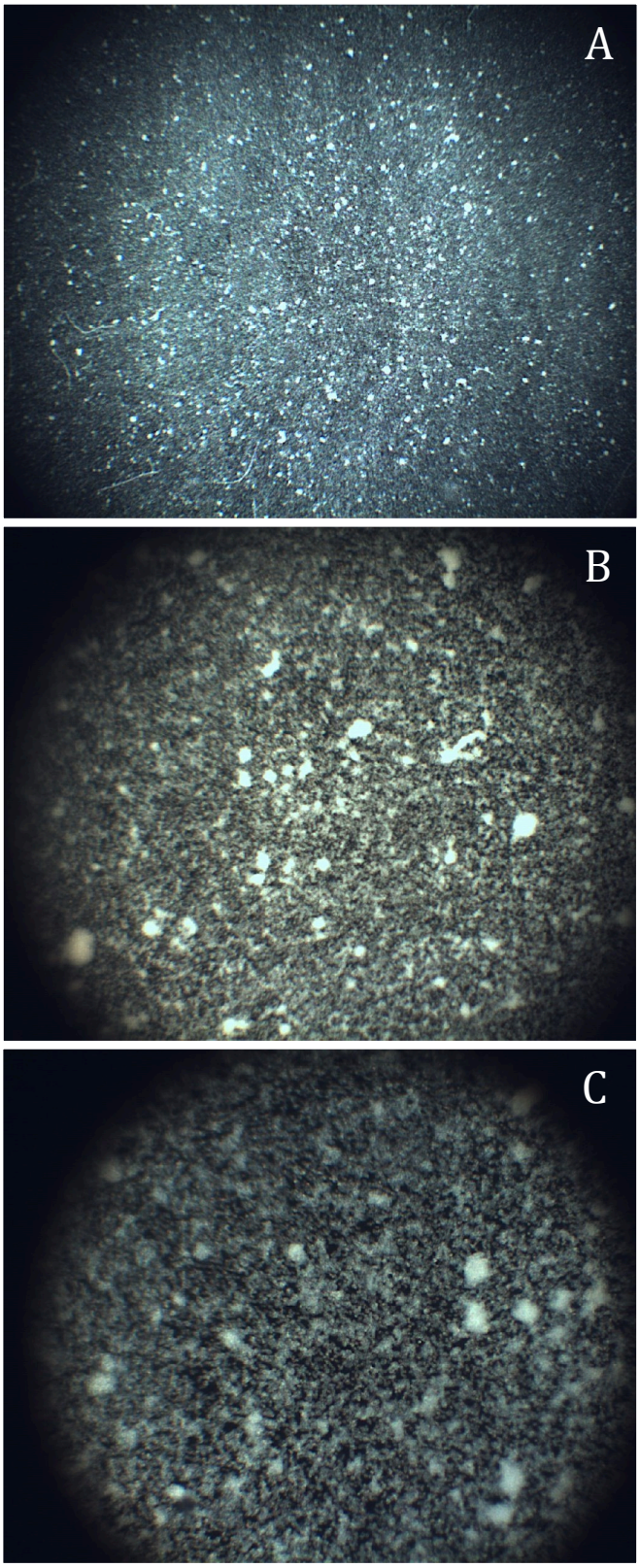

Fig. 14 shows the surface coverage achieved from this diamond solution was >80%. Importantly it appears the average size of the nanoparticles has decreased. It was previously found difficult to self-assemble nanodiamond less that 500nm onto metal substrates. However the technique described in sections 8.1 and 8.2 produced a reliable monolayer with <500nm diamond nanoparticles onto tungsten and tantalum substrates. The chemistry can be described as 'bucket chemistry' it is cheap, efficient, and most importantly it is commercially viable.

Figure 14 – *Optical Microscope images of Acid treated, Lithiated MSY Bac 441 HPHT re-filtered diamond particles assembled onto Tungsten substrates, pH 7.5. 10x(A), 50x(B), and 100x(C) Zoom. Good percentage coverage was achieved.*

Method: Wash substrates in KOH (40wt%) 30mins. Rinse with DI water. Submerge into PEI soln. (0.1wt%) 30mins. Rinse with DI water, dry under Argon. Pipette diamond solution (1wt%, pH7.5) onto substrate 1hr. Rinse (DI water). Dry under Argon.

8.3 Electrochemical Oxygenation of DNPs

Section 3.4 describes the oxygenation of diamond nanoparticles, and the uses in developing a positive electron affinity on the diamond surfaces. The two known methods of oxygenating diamond are thermal oxidation in a controlled furnace, and acid treatment. Acid treatment was used in this review to prepare diamond samples for self-assembly. However the level of oxygenation is not sufficient for use in thermionic emission testing.

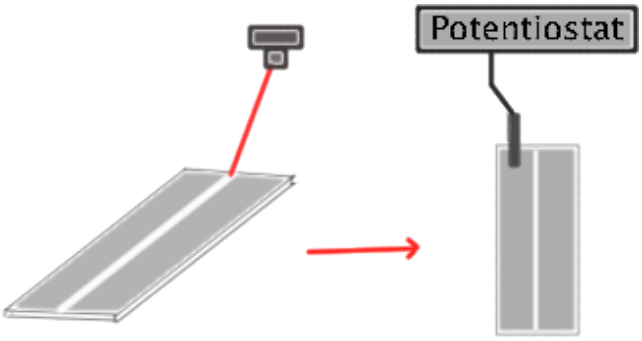

Figure 15 *– Sketch of the ITO preparation for electrochemical oxidation*

Electrochemistry has been seen in literature to oxygenate CVD diamond layers already assembled onto substrates. The electrochemical oxygenation of self-assembled diamond on ITO substrates demonstrated in this review is believed to be original.

As described in section 7.4, diamond self-assembled onto ITO electrodes was subjected to a cyclic range of voltages (0-5V) produce an oxidizing current. ITO glass electrodes were prepared by self-assembling nanodiamond onto the conducting ITO surface, as described in section 7.1. A laser was then used to cut a small slit up the centre of the electrode removing the diamond and ITO layer leaving only the glass exposed; stopping electrical conductivity between the two sides of the ITO electrode, see Fig. 15. This was in order to only oxidise one side of the electrode, so that a comparison could be made via SEM imaging. Consequently one side of the ITO was connected to the potentiostat and electrochemical oxidation was attempted.

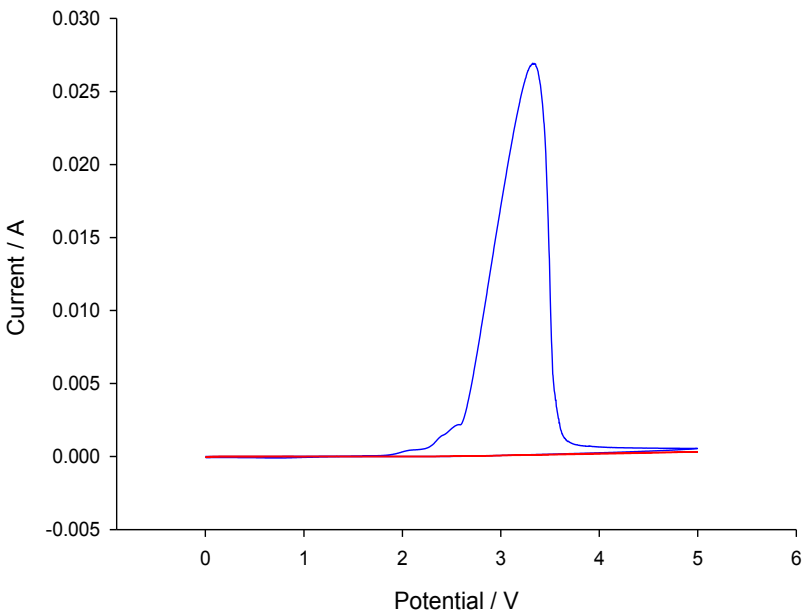

Figure 16 *– Cyclic voltammograms A (blue), B (red) of Acid washed, lithiated nanodiamond on ITO substrates.*

Fig. 16A shows a strong peak at a potential of 3V. This peak is not seen on a second scan (Fig.16B and Fig.17) of the same sample. The peak must therefore indicate the altering of the substrate, polymer, or the diamond inexorably. After running the sample through the potentiostat the surface diamond was visibly depleted and had been partially removed from the substrate surface. It is possible that the high potentials affect the polymer and therefore the diamond is no longer bound to the surface. A further cyclic voltammogram was run using plain ITO (shown in Fig.18). The peak at 3V is still visible. A possible conclusion of the circumstances faced is that the ITO layer is already in its highest oxidation state and under an oxidising current it cannot further oxidise, however the polymer solution irreversibly oxidises as shown by the peak at 3V. This reduces its cationic character and therefore its ability to keep the diamond held to the surface of the substrate.

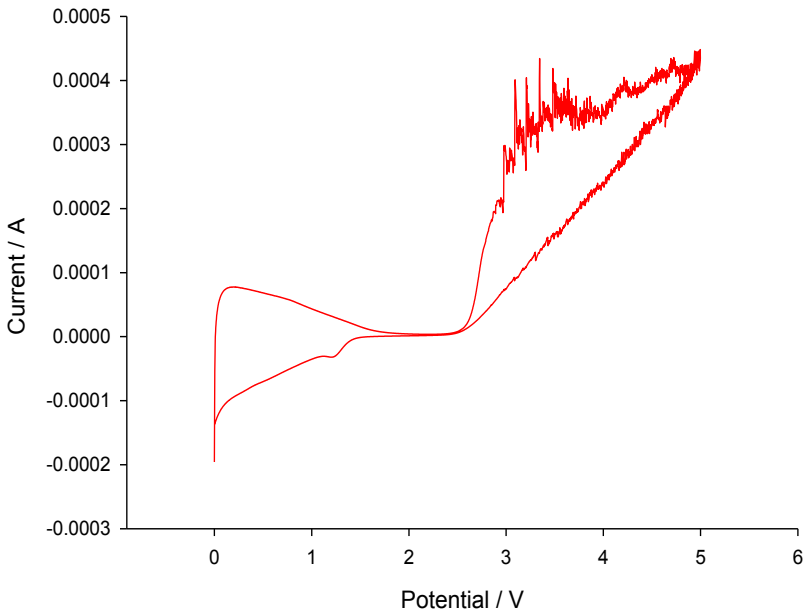

Figure 17 *– Cyclic voltammogram of Fig.16B. Acid washed, lithiated nanodiamond on ITO substrates. The 'noise' after 3V is possibly created by the liberation of hydrogen from the platinum counter electrode.*

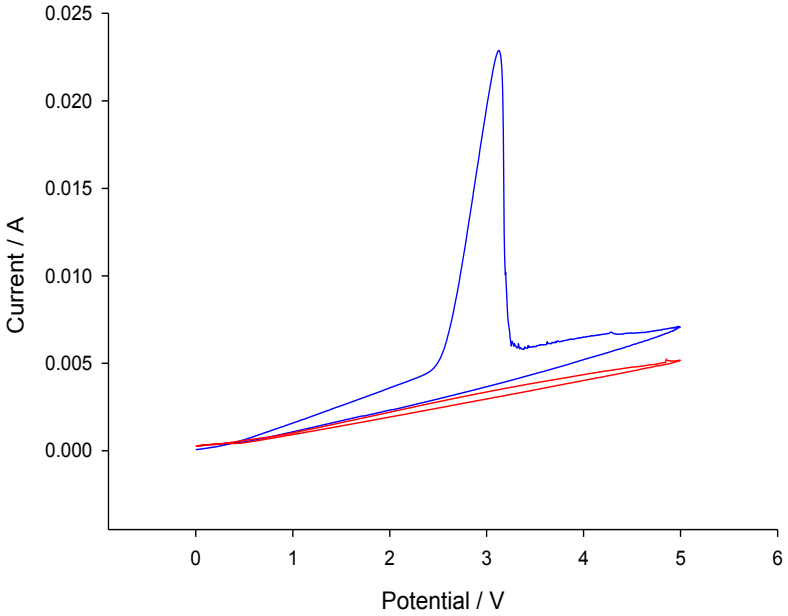

Figure 18 *– Cylic voltammogram, ITO electrode*

The diamond covered ITO electrodes were then annealed for future electrochemical testing to prevent the removal of diamond from the surface of the ITO. It was found that even the annealed nanodiamond was removed under potentials higher than 3V. The maximum potential of the proceeding cyclic voltammograms was kept below 3V. At this voltage the ITO did not produce a

large peak and the diamond stayed relatively in place. As the diamond was partially oxidised during the acid wash the alternative side of the ITO electrode was hydrogenated to give a fair comparison under the SEM. It is known that hydrogen terminated diamond particles glow/emit under the SEM; where as oxygenated diamond will look dull in comparison. When hydrogenated, as described in section 7.4, the diamond remained on the ITO, further suggesting that the polymer is susceptible to oxidation.

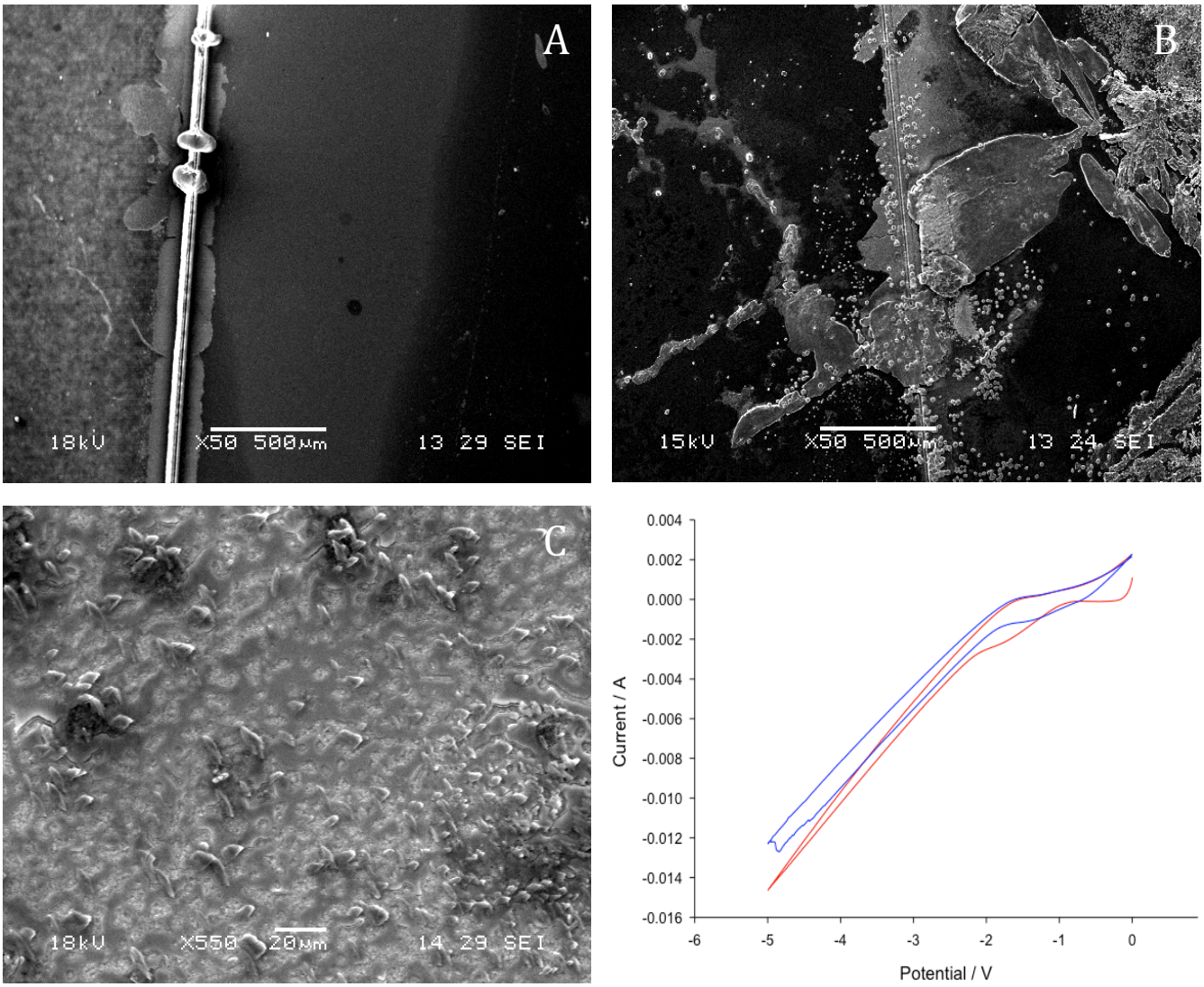

Figure 19 – *Shows SEM images (A, B and C) of acid washed, lithiated nanodiamond on ITO substrates. Fig.19A depicts Oxygenated diamond (at 5V) on the right side of the slit, with Hydrogenated diamond on the left. Most of the oxygenated diamond has been removed leaving plain ITO. Fig.19B is an SEM image of oxygenated diamond (at 5V on the right hand side of the slit and 3V on the left hand side). Fig.19C illustrates an annealed sample on ITO oxidised at 3V. The graph in Fig.19 shows a cyclic voltammogram of an ITO electrode up to-5V. No drastic peak is seen.*

Electrochemically oxidising the diamond particles below the 3V peak shown in Fig.18 where the PEI decomposes was more successful. However loss of diamond off the surface was still noticeable. Annealed samples remained intact, although as demonstrated in Fig.19C it appears the

polymer has liberated from the surface and engulfed the nanodiamond. Oxidation at these potentials remains difficult, although as described in section 10 it still remains fairly untested and could be a viable technique for oxidising diamond.

9.0 Conclusion

Diamond nanoparticles were self-assembled onto Tungsten and Tantalum substrates. The technique for self-assembly was revised to obtain the best percentage surface coverage, and reducing the aggregation of diamond on the surface. These substrates were analysed using an optical microscope and an SEM. The technique presented in sections 7.1 and 8.1 was concluded to be successful and greater than 80% coverage was achieved with minor aggregation. The process described could be used industrially. Tungsten substrates meant that high temperature vacuum annealing could take place, and therefore further thermionic testing.

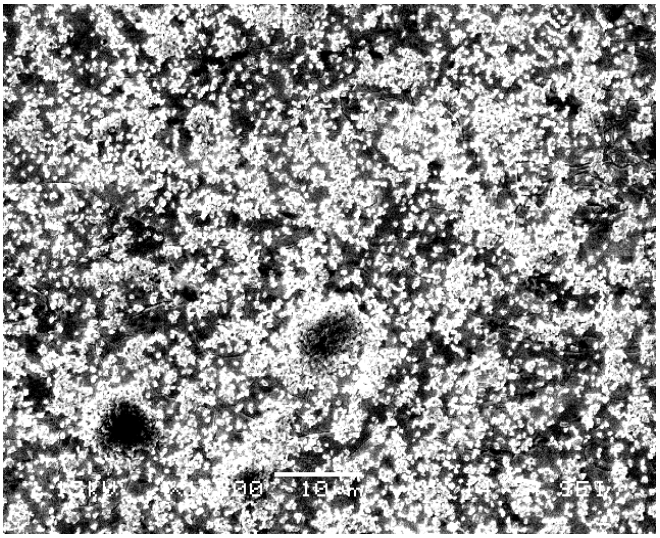

Figure 20 *– SEM image illustrating acid washed, lithiated diamond coverage on a tungsten substrate.*

A 450nm filter was used alongside fractional separation in order to reduce the size of the nanoparticles in solution, and aid thermionic emission. As Fig. 21 indicates, 300-400nm diamond particles were isolated successfully. It was found that these particles were more difficult to self-assemble, however >80% coverage was still achieved.

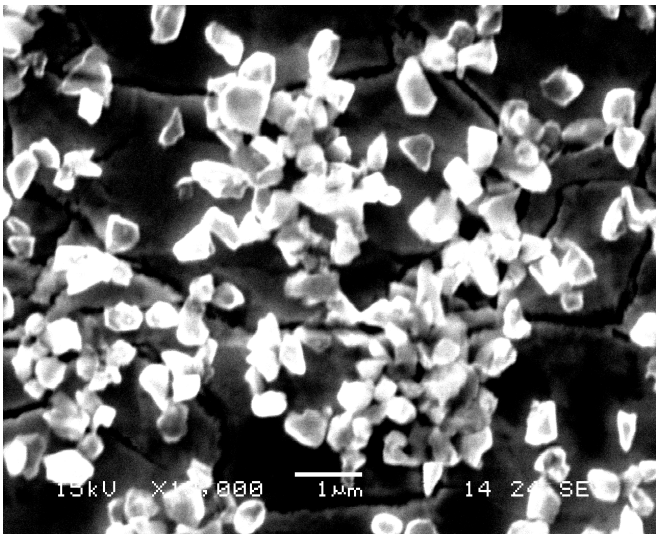

Figure 21 *– <450nm acid washed, lithiated diamond assembled onto a tungsten substrate.*

Oxygenation of diamond nanoparticles is highly important in the process of thermionic emission and therefore a commercially viable technique is required. Electrochemical oxidation is efficient and cheap. It has never, to the author's best knowledge, been used on self-assembled diamond particles. It was found that the high potentials used had a detrimental effect on the polymer, often removing the assembled diamond. This was made clear by a large peak at 3V appearing in cyclic voltammograms. Even after annealing and at potentials lower than 3V the polymer continued to fail.

10.0 Future work

It might be possible to use high temperature vacuum annealed samples on tungsten substrates for the electrochemical oxidation technique. This would allow for less reliance on the polymer to keep the diamond assembled onto the substrate surface.

In order to further reduce the particle size, complex centrifuge analysis could be undertaken. Analysing different cycle speeds, to calculate at what speeds do smaller particles remain in solution and larger (500nm) particles do drop out, isolating the smaller particles.

Due to the difficulty in obtaining thermionic emission from these samples it might be possible to change the substrates. Both the shape and topography of the substrate.

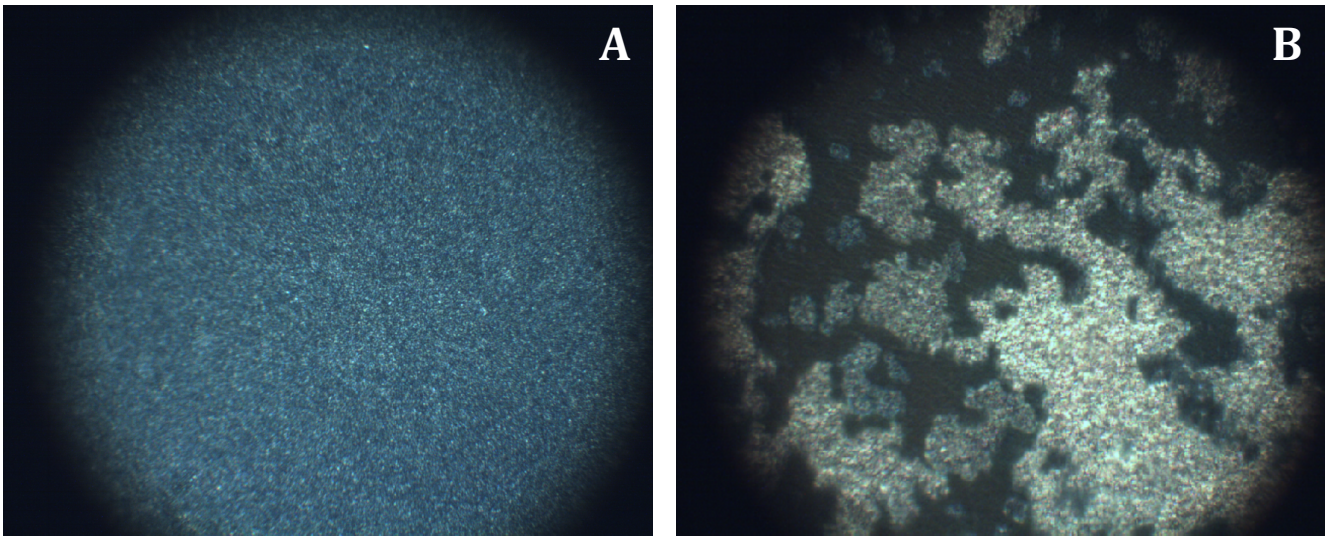

*Acid treated lithiated MSY Bac 441 HPHT diamond on Tungsten. (**A** – 10x zoom, **B** – 50x zoom). **A** displays good surface coverage, achieved with a pH 7.5, 1wt% diamond soln. **B** was produced with a pH 8, 2wt% soln.*

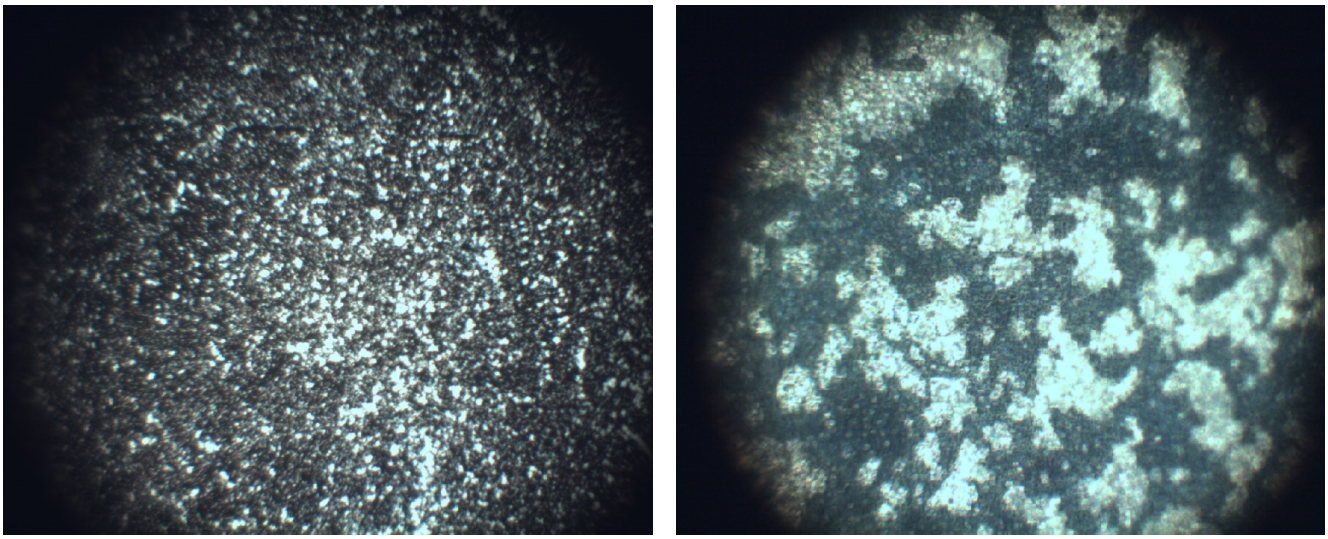

*Acid treated lithiated MSY Bac 441 HPHT diamond on Tungsten. (**C** – 10x zoom). (**D** – 50x zoom). Both samples were produced in the early stages of experimental procedure.*

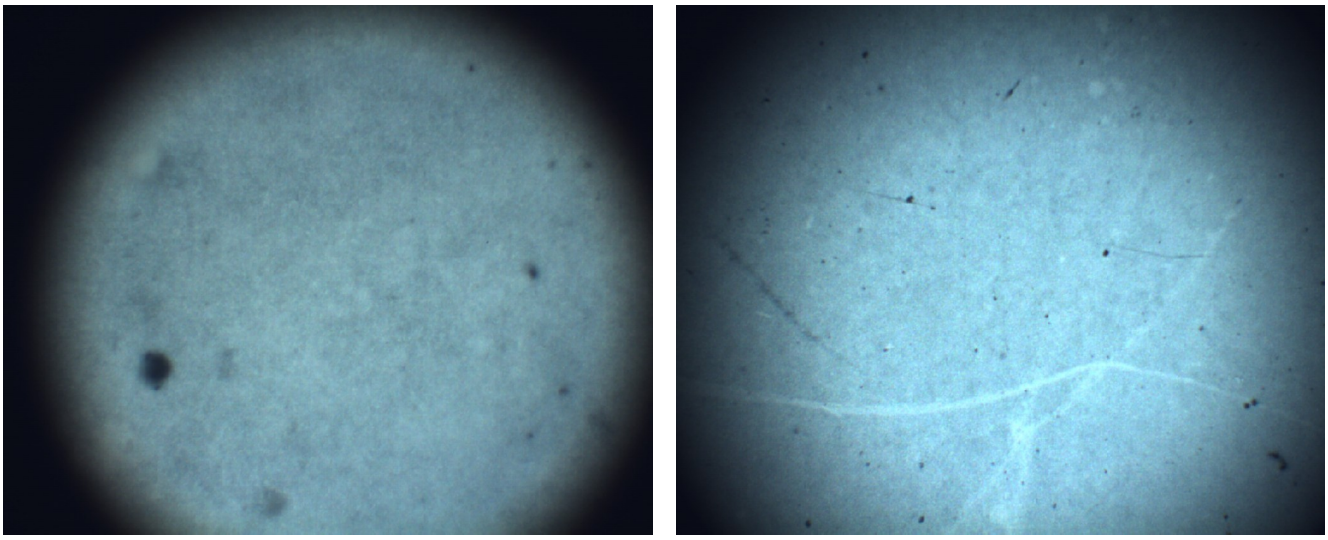

Acid treated lithiated MSY Bac 441 HPHT diamond on ITO. (E – 10x zoom). (F – 50x zoom). Samples were produced in testing of a known technique of self-assembly of diamond onto ITO.

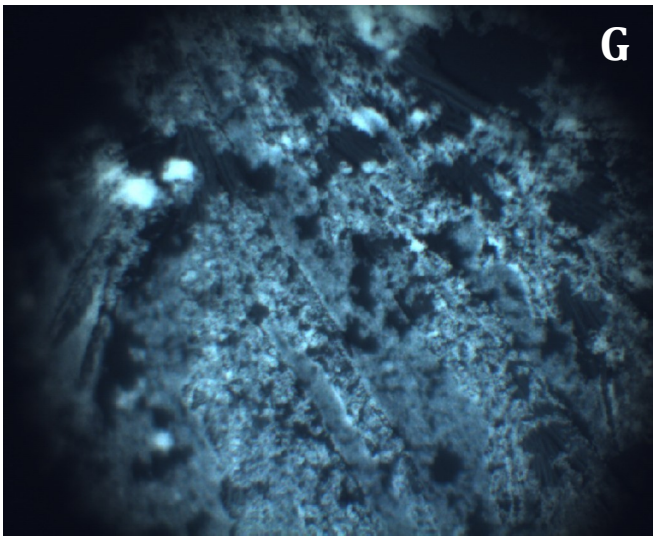

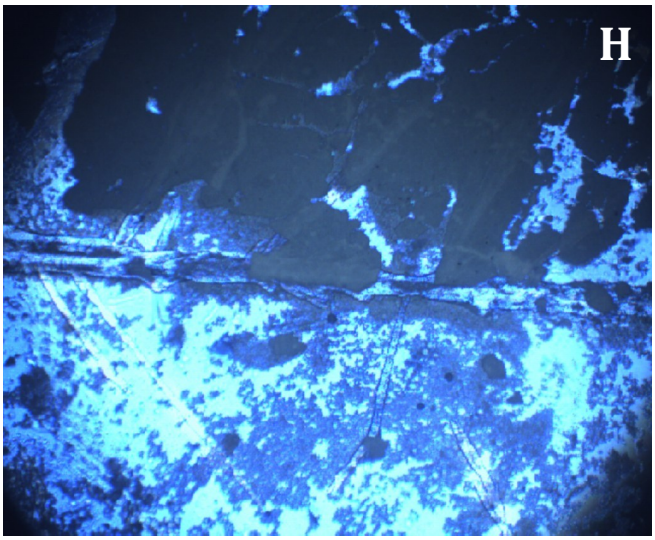

Acid treated lithiated MSY Bac 441 HPHT diamond on ITO. (G – 50x zoom). (H – 50x zoom). Attempted electrochemical oxidation observed. Destruction of PEI polmer clear.

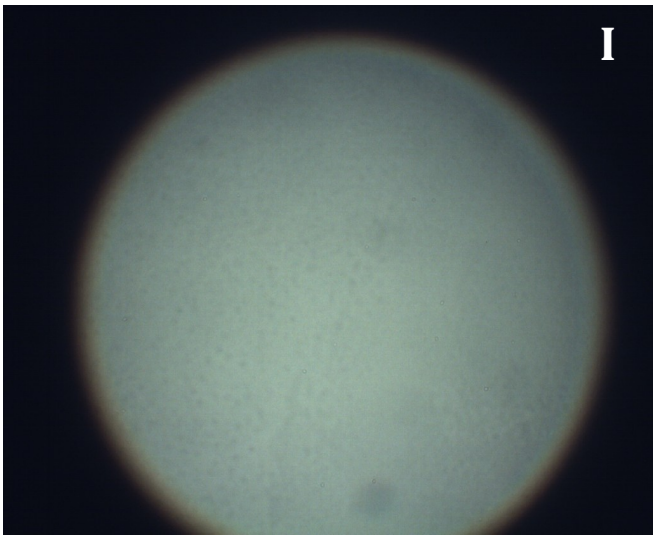

Acid treated lithiated MSY Bac 441 HPHT diamond on ITO. (I – 10x zoom).

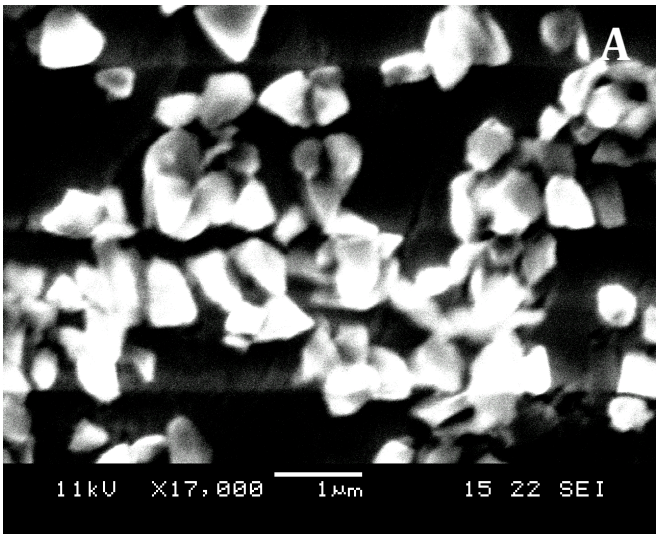

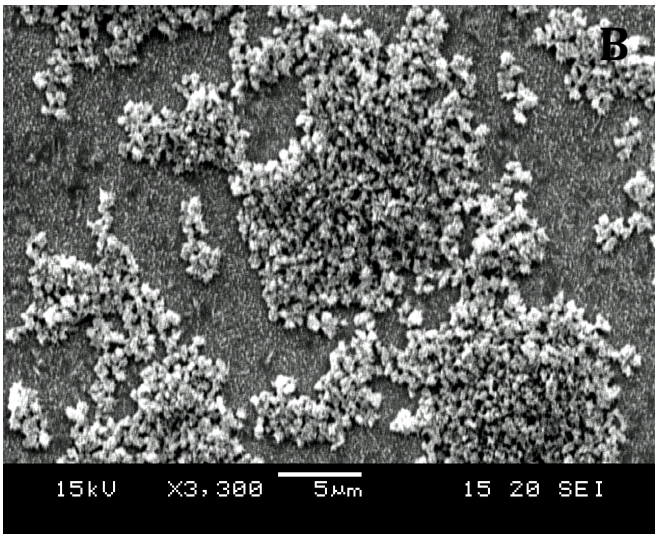

SEM of Acid treated lithiated MSY Bac 441 HPHT diamond on Tungsten. Early samples shown displaying a high level of aggregation. Diamond particles assembled ~500nm.

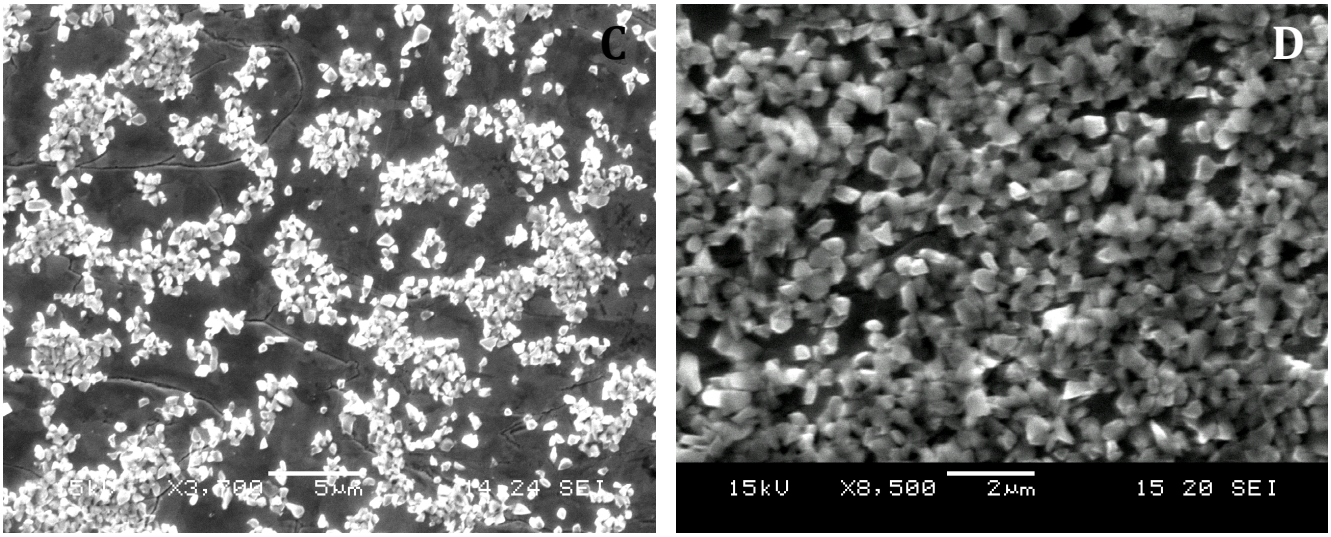

*SEM of Acid treated lithiated MSY Bac 441 HPHT diamond on Tantalum. Samples **C** and **D** display assembly of <450nm diamond on different scales.*

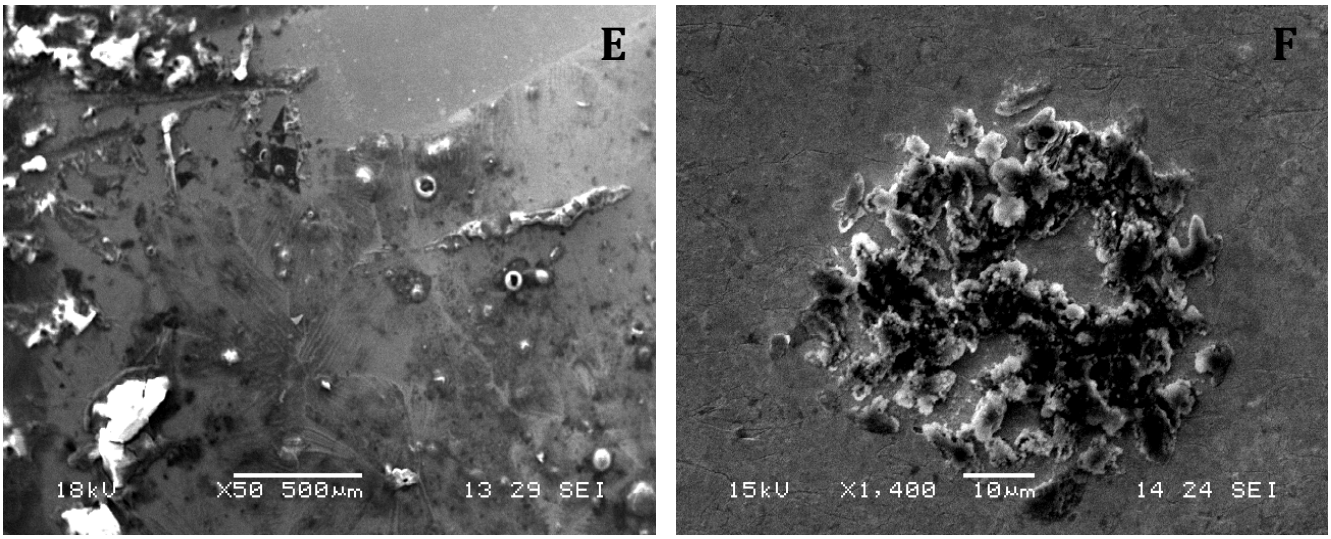

*SEM of Acid treated lithiated MSY Bac 441 HPHT diamond on ITO (sample **E**) and Tantalum (**F**). **E** shows the surface of ITO after electrochemical oxidation. **F** displays a' micellular' diamond formation.*

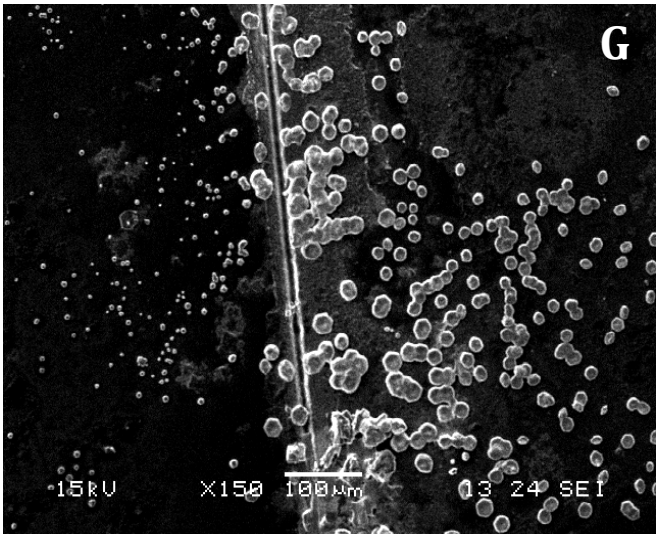

*SEM of Acid treated lithiated MSY Bac 441 HPHT diamond on ITO. The right side of sample **G** has been electrochemically hydrogenated. Whereas the left side has been electrochemically oxygenated.*

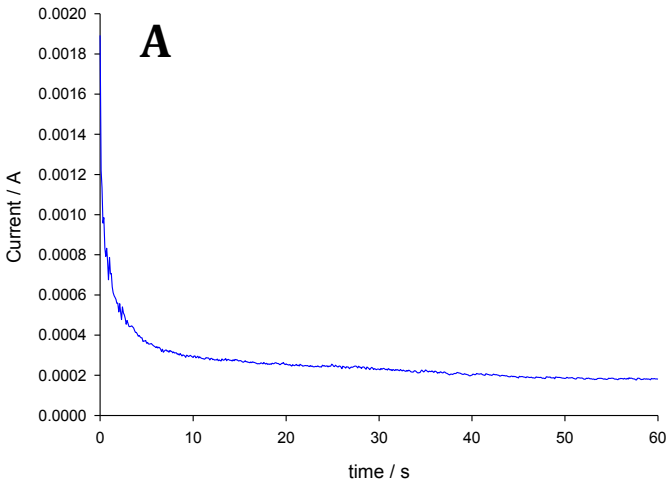

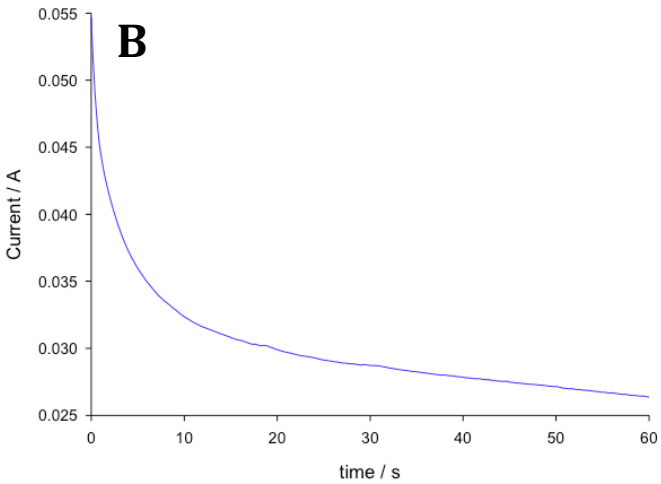

*Graphs **A** and **B** illustrate Chronoamperometry run at different currents.*

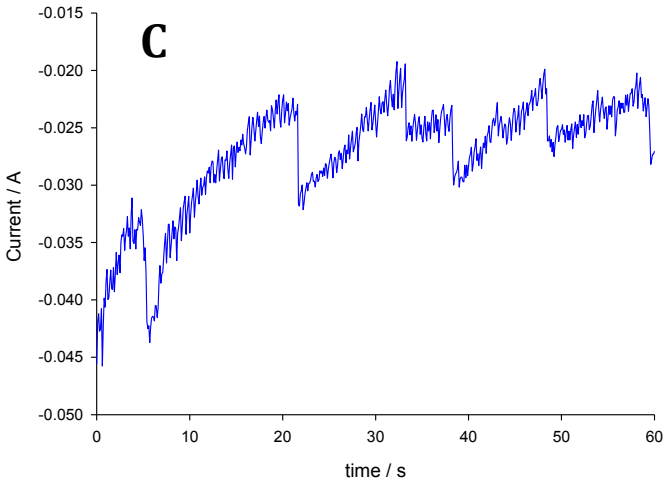

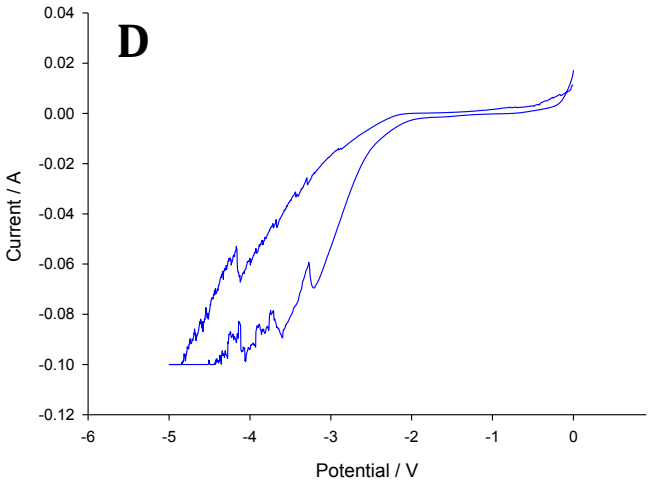

***C** displays a Chronoamperometry run at negative oxidizing currents the noise generated is from oxygen being liberated at the platinum counter electrode. **D** shows cyclic voltammetry down to a potential of -5V.*

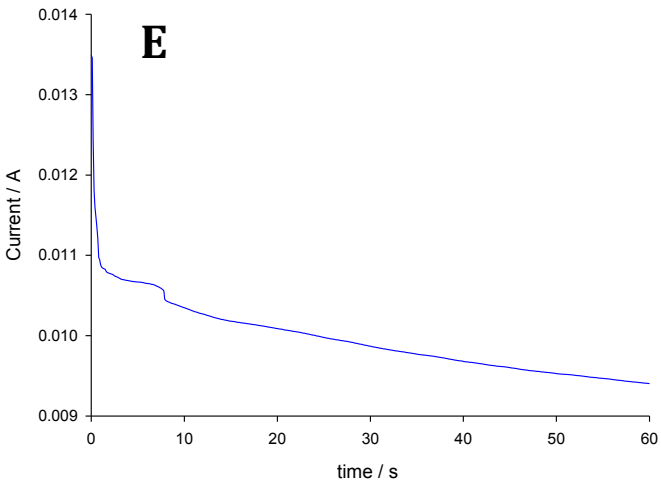

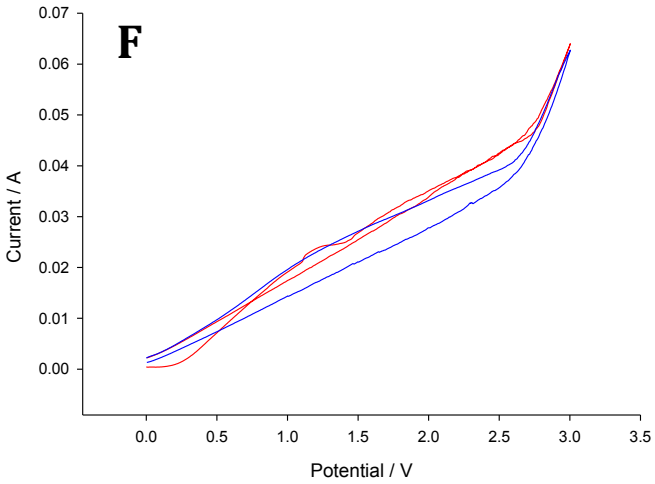

*Further Chronoamperometry (**E**) and cyclic votlammetrey (**F**) results.*

[1] Nobel Lectures, Chemistry 1922-1941; I. Langmuir 1932

[2] P. W. May; *Phil. Trans. R. Soc. Lond. A*; 2000, **348**, p473-495
[3] O. A. Shenderova; *Crit. Rev. Sol. State Mater. Sci*; 2002, **27**, p227-356
[4] A. Krueger; *Adv. Mater*; 2008, **20**, p2445-2449
[5] O. A. Shenderova, D. M. Gruen; *Ultrananocrystalline Diamond*; pub:2006, Norwich, UK
[6] F. Pacheco-Torgal, S. Jalali; *Construction & Building Mater*; 2011, **25**, p582-590
[7] R. Feynman; '*There's plenty of room at the bottom' Speech given at the AGM of the Americal Phys. Soc.*; 1960, **23**, p22-36
[8] N. Taniguchi; *Int. Conference Production Engineering Tokyo*; 1974, **2 (II)**, p18-23
[9] K. B. Holt; *Phil. Trans. R. Soc. A*; 2007, **365**, p2845-2861
[10] H. Ishizaka, et al; *Diamond Rel. Mater*; 2003, **12**, p1800-1803
[11] O. A. Williams, et al; *Chem. Phys. Lett*; 2007, **445**, p255-258
[12] K. B. Holt; *Phil. Trans. R. Soc. A*; 2007, **365**, p2845-2861
[13] J. H. Fendler; *Chem. Mater*; 2001, **13**, p3196-3210
[14] S. Mann; *Nature*; 1988, **332**, p119
[15] S. Mann; *Mineralization in Biological Systems*; 1983, p125
[16] C. Viney; *Supramolecular Sci*; 1997, **4**, p75-81
[17] L. Addadi, S. Weiner; *Angew. Chem*; 1992, **31**, p153
[18] Nobel Lectures, Chemistry 1922-1941; I. Langmuir 1932
[19] I. R. Peterson; *J. Phys*; 1990, **23**, p379
[20] K. Graf, H. Riegler; *Langmuir*; 2000, **16**, p5187
[21] K. Blodgett, I. Langmuir; *Phys. Rev*; 1937, **51**, p965-967
[22] I. R. Peterson; *J. Phys*; 1990, **23**, p379
[23] J. H. Fendler; *Chem. Mater*; 2001, **13**, p3196-3210
[24] S. B. Velegol, et al; *Langmuir*; 2000, **16**, p2548-2556
[25] G. Decher, et al; *Thin Solid Films*; 1992, **210/211**, p831-835
[26] L. Ferrari, et al; *J. Colloid and Interface Sci*; 2010, **347**, p15-24
[27] J. H. Fendler; *Chem Mater*; 1996, **8**, p1616-1624
[28] W. Bigelow, et al; *J. Colloid Sci*; 1946, **1**, p513-538
[29] A. Ulman; *Chem. Rev*; 1996, **96**, p1533-1554
[30] R. G. Nuzzo, D. L. Allara; *J. Am. Chem. Soc*; 1983, **105**, p4481-4483
[31] N. Tillman, et al; *Langmuir*; 1989, **5**, p101-111
[32] M. A. Ratner, et al; *J. Am. Chem. Soc*; 1990, **112**, p7389-7390
[33] M. Pomerantz, et al; *Thin Sol. Films*; 1985, **132**, p153-162
[34] J. H. Fendler; *Chem. Mater*; 2001, **13**, p3196-3210
[35] L. Daikhin, et al; *Anal. Chem*; 2002, **74**, 554-561
[36] Röseler. A; *Thin Solid Films*; 1993,
[37] F. M. Hoffmann; *Surface Sci. Rep*; 1983, **3**, p107-192
[38] V.V. Danilenko; *Phys. of the Sol. State*; 2004, **46**, p595-599
[39] M. Akaishi, et al; *J. Crystal Growth*; 1990, **104**, p578-581
[40] G. Burkhard et al; *Appl. Phys. Lett*; 1995, **23**, p3131-3133
[41] L. F. Trueb; *J. Appl. Phys*; 1968, **39**, p4707
[42] A. Krueger; *Adv. Mater*; 2008, **20**, p2445-2449
[43] O. A. Shenderova; *Crit. Rev. Sol. State Mater. Sci*; 2002, **27**, p227-356
[44] Y. Hirose, Y. Terasawa; *Jpn. J. Appl. Phys*; 1986, **25**, p519-521
[45] P. W. May; *Phil. Trans. R. Soc. Lond. A*; 2000, **348**, p473-495
[46] E. A. Ekminov, et al; *Nature*; 2004, **428**, p542-545
[47] J.E. Field; *The Properties of Natural and Synthetic Diamond*; New York: Academic ed., 1992
[48] P. W. May; *Phil. Trans. R. Soc. Lond. A*; 2000, **348**, p473-495
[49] A. M. Schrand, et al; *Crit. Rev. Solid State Mater. Sci*; 2009, **34**, p18-74
[50] R. Kalish; *J. Phys. D: Appl. Phys*; 2007, **40**, p6467-6478

[51] R. Kalish; *Diamond Rel. Mater*; 2001, **10**, p1749-1755
[52] E. A. Ekminov, et al; *Nature*; 2004, **428**, p542-545
[53] V. S. Robinson, et al; *Diamond Rel. Mater*; 2008, **15**, p1601-1608
[54] J. D. Rameau, et al; *Phys. Rev. Lett*; 2011, **106**, p137602(1-4)
[55] M. Panizza, G. Cerisola; *Electrochim. Acta*; 2005, **51**, p191-199
[56] R. Kalish; *Carbon*; 1999, **37**, p781-785
[57] G. Braunstein, R. Kalish; *Appl. Phys. Lett*; 1981, **38**, p416
[58] S. A. Kajihara, A. Antonelli, J. Bernholc; *Phys. Rev. Lett*; 1991, **66**, p2010
[59] T. L. Martin, et al; *MRS Proceedings*; 2011, **1282**, p449
[60] A. Krueger; *Adv. Mater*; 2008, **20**, p2445-2449
[61] R. Müller, A.Denisenko, M. Adamschik, E. Kohn; *Diamond Rel. Mater*; 2002, **11**, p651
[62] A. S. Barnard, M. Sternberg; *Diamond Rel. Mater*; 2007,**16**, p2078-2082
[63] H. Yamaguchi, et al; *Phys Rev*; 2009, **80**, p165321(1-5)
[64] P. W. May, et al; *Diamond Rel. Mater*; 1998, **7**, p671-676
[65] F. Maier, J Restein, L. Ley; *Phys. Rev. B*; 2001, **61**, p165411
[66] R. Hoffmann, et al; *App. Phys. Lett*; 2010, **97**, p52103(1-3)
[67] L. Diederich, et al; *Surface Sci*; 1999, **424**, p314-320
[68] M. C. Salvadori, et al; *Diamond Rel. Mater*; 2010, **19**, p324-328
[69] H. J. Looi, et al; *Diamond Rel. Mater*; 1998, **7**, p550-555
[70] K. Hayashi, S. Yamanaka, H. Okushi, K. Kajimura; *App. Phys. Lett*; 1996, **68**, p376
[71] K. Ishizaka, et al; *Phys. Rev. Lett*; 2008, **100**, p166402(1-4)
[72] F. Maier, J Restein, L. Ley; *Phys. Rev. B*; 2001, **61**, p165411
[73] C. E. Nebel, B. Rezek, D. Shin, H. Watanbe; *Phys. Stat. sol (a)*; 2006, **203**, p3273-3298
[74] K. M. O'Donnell, T. L. Martin, N. A. Fox, D. Cherns; *Phys. Rev. B*; 2010, **82**, p115303(1-9)
[75] V. Chakrapani, et al; *Science*; 2007, **318**, p1424-1430
[76] W. Hongthani, N. A. Fox, D. J. Fermin; *Langmuir*; 2011, **27**, p5112
[77] J. Hees, A. Kriele, O. A. Williams; *Chem. Phys. Lett*; 2011, **509**, p12
[78] O. A. Williams, et al; *Chem. Phys. Lett*; 2010, **495**, p84-89
[79] K. B. Holt; *Phil. Trans. R. Soc. A*; 2007, **365**, p2845-2861
[80] V. S. Bondar, I. O. Pozdnyakova, A. P. Puzyr; *Phys. Solid State*; 2004, **46**, p588-560
[81] T. M. Allen, P. R. Culis; *Science*; 2004, **303**, p1818-1822
[82] H. Huang, E. Pierstorff, E. Osawa, D. Ho; *Nano Lett*; 2007, **7**, p3305-3314
[83] N. G. Portney, M. Ozkan; *Anal. Bioanal. Chem*; 2006, **384**, p620-630
[84] O. C. Farokhzad, et al; *Proc. Natl. Academy Sci U.S.A*; 2006, **103**, p6315-6320
[85] L. C. Lora Huang, H-C. Chang; *Langmuir*; 2004, **20**, p5879-5884
[86] A. P. Puzyr', I. O. Pozdynakov, V. S. Bondar; *Phys. Solid State*; 2004, **46**, p761-763
[87] A. Gruber, et al; *Science*; 1997, **276**, p2012-2014
[88] J. R. Mansfield, K. W. Gossage, C. C. Hoyt, R. M. Levenson; *J. Biomed. Opt*, **10**, p041207
[89] K. B. Holt; *Phil. Trans. R. Soc. A*; 2007, **365**, p2845-2861
[90] C-C. Fu, et al; *Proc. Natl. Academy Sci U.S.A*; 2007, **104**, p727-732
[91] V. Y. Dolmatov; *Russian Chem. Rev*; 2001, **70**, p607
[92] K. Ueda, et al; *IEEE Electron Device Lett*; 2006, **27**, p570-572
[93] P. W. May; *Phil. Trans. R. Soc. Lond. A*; 2000, **348**, p473-495
[94] P. R. Chalker, C. Johnston; *Phys. Stat. Sol*; 1996, **54**, p455
[95] P. W. May; *Phil. Trans. R. Soc. Lond. A*; 2000, **348**, p473-495
[96] H. Ishizaka, et al; *Diamond Rel. Mater*; 2003, **12**, p1800-1803
[97] O. A. Williams, et al; *Chem. Phys. Lett*; 2007, **445**, p255-258
[98] S. Mandal, et al; *Nanotechnology*; 2010, **21**, p195303(1-4)
[99] S. Mandal, et al; *ACS Nano*; 2011, **5**, p7144-7148
[100] C. Wang, A. Garcia, D.C. Ingram, M. Lake, M.E. Kordesch; *Electronics Lett*; 1991, **27**, p1459-1461
[101] J. S. Lee, K. S. Lui, I. N. Lin; *App. Phys. Lett*; 1997, **71**, p554-556

[102] T. Tyler, V. V. Zhirnov, A. V. Kvit, D. Kang, J. J. Hren; *App. Phys. Lett*; 2003, **82**, p2904-2906
[103] A. Hamnett; *Catalysts Today*; 1997, **38**, p445-457
[104] X. Lu, J. Hu, J. S. Foord, Q. Wang; *J. Electroanal. Chem*; 2011, **654**, p38-43
[105] G. R. Salazar-Banda, K. I. B. Eguiluz, L. A. Avaca; *Electrochem. Com*; 2007, **9**, p59-64
[106] W. Zhao, J-J. Xu, Q-Q. Qui, H-Y. Chen; *Biosens. & Bioelec*; 2006, **22**, p649-655
[107] M. C. Granger, J. Xu, J. W. Strojek, G. M. Swain; *Anal. Chimica Acta*; 1999, **397**, p145-161
[108] G. Materlik; *Chem. Commun*; 2003, **10**, p1021-1023
[109] V. A. Koryukin; *Atomic Energy*; 2001, **90**, p1
[110] M. S. El-Genk, Y. Momozaki; *Energy Conversion & Mgmt*; 2002, **43**, p911
[111] J. Alvarez-Ramirez, H. Puebla, G. Espinosa; *Annals of Nuclear Energy*; 2001, **28**, p93-112
[112] F. A. M. Koeck, R. J. Nemanich; *Diamond and Rel. Mater*; 2006, **15**, p217-220
[113] R. Forman; *Int. Electron Devices Meeting*; 1991, **8-11**, p387-390
[114] F. A. M. Koeck, et al; *Diamond and Rel. Mater*; 2011, **20**, p1229-1233
[115] Y. V. Pleskov, et al; *J. Electroanal. Chem*; 1987, **228**, p19
[116] G. M. Swain; *Adv. Mater*; 1994, **6**, p388-392
[117] Y. V. Pelskov; *Russian J. Electrochem*; 2002, **38**, p1275-1291
[118] M. Hupert, et al; *Diamond Rel. Mater*; 2003, **12**, p1940-1949
[119] R. L. McCreery; *Chem. Rev*; 2008, **108**, p2646-2687
[120] M. Panizza, G. Cerisola; *Electrochim. Acta*; 2005, **51**, p191-199
[121] R. L. McCreery; *Chem. Rev*; 2008, **108**, p2646-2687
[122] M. C. Granger, et al; *Anal. Chem*; 2000, **72**, p3793-3804
[123] R. Hoffmann, et al; *Langmuir*; 2012, **28**, p47-50
[124] R. Hoffmann, et al; *App. Phys. Lett*; 2010, **97**, p052103